THE FIRST PRINCIPLE CALCULATIONS ON THE STRUCTURAL, MECHANICAL, AND ELECTRONIC PROPERTIES OF $KMnF_3$ AND $SrMoO_3$ PEROVSKITE COMPOUNDS

BY

GODRICA ONOTASAMIDERHI

PSC1709286

DEPARTMENT OF PHYSICS,
FACULTY OF PHYSICAL SCIENCES,
UNIVERSITY OF BENIN,
BENIN CITY.

DECEMBER, 2022.

THE FIRST PRINCIPLE CALCULATIONS ON THE STRUCTURAL, MECHANICAL, AND ELECTRONIC PROPERTIES OF $KMnF_3$ AND $SrMoO_3$ PEROVSKITE COMPOUNDS

BY

GODRICA ONOTASAMIDERHI

PSC1709286

A PROJECT WORK SUBMITTED TO THE DEPARTMENT OF PHYSICS, FACULTY OF PHSYICAL, UNIVERSITY OF BENIN, IN PARTIAL FULFILMENT OF THE REQUIREMTNS FOR THE AWARD OF BACHELOR OF SCIENCE (B.SC. HONS) DEGREE IN PHYSICS.

DECEMBER, 2022.

CERTIFICATION

This is to certify that the project work titled **'**the first principle calculations on the structural, mechanical, and electronic properties of $kmnf_3$ and $srmoo_3$ perovskite compounds' **w**as carried out by GODRICA ONOTASAMIDERHI with matriculation number PSC1709286 in the Department of Physics, Faculty of Physical Sciences, University of Benin

_____ **_____**

DR. IYORZOR BEN. **DATE**
Project Supervisor

_____ **_____**

PROF. O. D. OSAHON (Ph.D.). **DATE**
Head of Department

_____ **_____**

EXTERNAL EXAMINER **DATE**

DEDICATION

This project work is dedicated to the ALIMIGHTY GOD the author and the finisher of my faith with whom all things are possible and my father Dr. RAYMOND BENSON and SIBLINGS for their uncompromising and relentless support in my academics pursuit.

CERTIFICATION OF DISSERTATION ON PLAGIARISM

We the undersigned attest and declare that the dissertation of GODRICA ONOTASAMIDERHI titled **'**the first principle calculations on the structural, mechanical, and electronic properties of $kmnf_3$ and $srmoo_3$ perovskite compounds' **w**as carried out has successfully passed the anti-plagiarism test and doesn't violate any copyright

DR. IYORZOR BEN. **DATE**
Project Supervisor

PROF. O. D. OSAHON (Ph.D.). **DATE**
Head of Department

ACKNOWLEDGEMENT

I return all Glory to God, for his grace of accomplishment to complete this project with his unending and unflinching strength made available to me during the course of making this project wholly.

I would like to express my unending gratitude to my sapient supervisor, Dr. B.E IYORZOR for his applicable guidance, support and ideas in completing this project. I would like to thank the Department of Physics for the opportunities to perform the project successfully.

Special appreciation to my parents Mr. Raymond Benson & Mrs Rosemary Benson for their love and support towards my academics pursuit.

Also, this project work won't be complete if I don't acknowledge Dr. Maureen, her love, care and support drove me through the years in school.

Finally, I would like to use this opportunity to acknowledge and thank my friend, BLESSING UMOREN for her support all through this period.

TABLE OF CONTENTS

LIST OF FIGURES

LIST OF TABLES

ABSTRACT

Density functional theory calculations have been carried out on the Structural, Mechanical and Electronic Properties of $KMnF_3$ and $SrMoO_3$ Perovskite Materials based on the Density Functional Theory (DFT) by using the Ultra Soft Pseudo Potential (USPP) from the Quantum Expresso (QE) software program.

The generalized gradient approximation of Perdew-Burke-Ernzerhof (GGA) is used in the calculation of total energy. The lattice constant of both compounds are well optimized. The calculated equilibrium lattice parameters, band structures, elastic constants and the elastic moduli of both $KMgF_3$ and $SrMoO_3$ perovskite compounds are in good agreement with theoretical results. Furthermore, I was able to obtain the Density of State and Band structure graphs for both compounds to determine their electronic properties.

We have employed first principle calculation pseudopotential method, within a generalized gradient approximation of the density functional theory, a linear response approach, to determine structural, mechanical and electronic properties of the $KMgF_3$ and $SrMoO_3$ perovskite compounds. The obtained structural and elastic parameters are in good agreement with previous experimental and theoretical results. The analysis of B/G ratio indicates that both $KMnF_3$ and $SrMoO_3$ is a ductile material.

CHAPTER ONE

INTRODUCTION

1.1 PEROVSKITES COMPOUNDS

Perovskites is a well-known and widely studied family of materials with a variety of applications in everyday life. The early perovskite materials had the general structure of ABO3. A had to be a cation of +2 valence and B a cation of +4 valence in order to achieve charge neutrality (Pena, M.A.; Fierro, J.L., 1981). They have CaTiO3 as chemical formula, it obtains its name from mineral named as a calcium titanium oxide and it revealed by Gustav Rose in the Ural Mounts of Russia. The name Perovskite came after Lev Perovski (1792–1856) who was the first discoverer in 1792 (Cheng and Lin, 2010). Its crystal was first described in 1926 (Wenk andBulakh, 2004) and published in 1945 (Szuromi and Grocholski, 2017).

ABX3 is the main formula for all Perovskite compound. In this formaula A and B are two cations of very dissimilar bulks (Atta et al., 2016), C is an octahedron ions surrounded the B ion and X is an anion that bonds to both (Schaak and Mallouk, 2000). X is often oxygen and other big ions such as halides, sulfides and nitrides are probable. Numerous oxide compounds are known belonging to

a few perovskite-based homologous series (Tsunoda et al., 2003).

Perovskite oxides types (in their ideal form) are cubic or nearly cubic in structure like other transition metal oxides which contains the same formula (ABO3). At low temperature some phase transitions may be occurs. Oxides class of compounds has wide potential for many uses due to their structures crystal which are simple and

exceptional in their ferroelectric and dielectric properties.

Perovskites structures material exist in three types; the first one contain localized electrons, the second contains delocalized energy-band states, while the third can be a transition between these two types (Szuromi and Grocholski, 2017). There are several of perovskites structures types that exists in different form such as:

A2BO4 Layered perovskite, ABO3-perovskite, A2A0B2B0O9 Triple perovskite and A2BB0O6 Double perovskite, etc. (Thomas et al., 2017), the most abundant ones are MgSiO3 and FeSiO3.

In solid-state physics, perovskite oxides have been studied because they put up most of the metal ions in the periodic table due to its substantial number of different anions (Nagata et al., 2013). These types of solids are significant in the field of electrical ceramics such as; material science, astrophysics, particle

accelerators (Zhu et al., 2014) geophysics, fission-fusion reactors (Nagata et al., 2013), refractories, heterogeneous catalysis environment (Seyfi et al., 2009), etc.

Oxides and oxides-like types of perovskite have different properties such as; insulator-metal transition, ionic conduction characteristics, dielectric, variation of solid-state phenomena, metallic, and superconducting characters, it also have many applications in physics and chemistry filed (Kreisel et al., 2000).

Perovskite-structured oxides can accept considerable substitutions in one or both cationic sites (A and B sites) while retaining their original crystal structures (Xu et al., 2009). Recently, perovskite-structured ceramics have several extraordinary applications such as random access memories (Pengfei et al., 2017), actuators, tunable microwave devices displays (Nenasheva et al., 2004), piezoelectric devices (Protesescu et al., 2015), transducers, wireless communications (Muralt et al., 2009), sensors, and capacitors (Kawamura et al., 2002).

In several applications perovskites proved to have great interest due to their useful properties in surface acoustic wave signal processing devices, electrochromic, switching, image storage, filtering, and photochromic (Atta et al., 2016). Recently, halide perovskites have drawn considerable attention in the

fields of material exploration (Pengfei et al., 2017) due to its great effectiveness of solid-state solar.

1.2 AIMS AND OBJECTIVES

This research aims to conduct a first principle study on $KMnF_3$ and $SrMoO_3$ perovskite compounds.

1.3 OBJECTIVES

The objectives are to calculate the;

1. Structural properties.
2. Mechanical properties (Elastic Constant, Bulk Modulus, Shear Modulus, Young Modulus).
3. Electronic properties (Band Gap, Density of State, Material Type).

CHAPTER TWO

LITERATURE REVIEW

2.1 STRUCTURE OF PEROVSKITES

Perovskite or perovskite-structure are used interchangeably. This name is given to anything has the generic form ABX3 and the same crystallographic structure. True perovskite is formed from oxygen, titanium and calcium, in the form CaTiO3 (Bradley, 2017; Jeon et al., 2015). Also it referred to a kind of ceramic oxides having ABX formula. These compounds are classified into alkaline metal halide Perovskites, inorganic oxide perovskites, and organic metal halide perovskites (Chen et al., 2018).

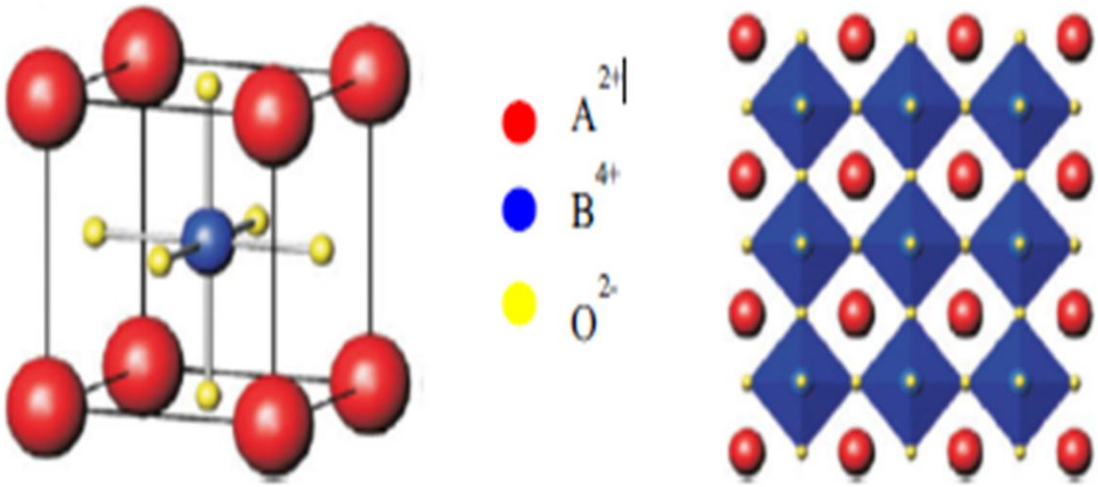

Fig. 1: Ideal cubic perovskite structure (ABO_3)

The perovskite materials have a common structure termed as ABX3, where ‘‘A” and ‘‘B” are cations have different sizes and ‘‘X” is an anion which bonds to both. The ‘A’ atoms are bigger than the ‘B’ atoms (Ono et al., 2017). The A and B locations may be replaced by any metal or semimetal from the periodic table. In all cases, the anion is oxygen, and can be any other could be found at this position (Chen et al., 2018).

The perovskite materials have a common structure termed as ABX3, where ‘‘A” and ‘‘B” are cations have different sizes and ‘‘X” is an anion which bonds to both. The ‘A’ atoms are bigger than the ‘B’ atoms (Ono et al., 2017). The A and B locations may be replaced by any metal or semimetal from the periodic table. In all cases, the anion is oxygen, and can be any other could be found at this position (Chen et al., 2018).

The atomic arrangements in perovskite structure are the first found for the mineral perovskite calcium titanate, it have submetallic to metallic luster cube like-structure beside deficient cleavage and hard tenacity, colorless streak or colors include orange, black, brown, yellow and gray (Whitfield et al., 2016; Yi et al., 2019).

Ideally, the perovskite structure is described as cubic. The A atoms form the corners of the cubic cells, B atoms are in the centre in 6-fold coordination, surrounded by an octahedron of anions, the oxygen atoms are situated in the faces’ centres, and the A cation in 12-fold cub- octahedral coordination.

In perovskite cubic unit cell (Fig. 1), atom A ion is a lanthanides with larger radius or alkali earth metals (Khajonrit et al., 2018). Generally, A cations are 12 fold coordinated by oxygen anions and sits in corners of the cube at corner position (0, 0, 0) while oxygen atoms are at the face center of the cubic lattice at position (½, ½, 0) but tetravalent B cations lie within oxygen octahedral, occupies the body center position (½, ½, ½). The structure is pictured as a three dimensional network of regular corner linked BO6 octahedral (Tan et al., 2014). The general formula as ABO3 where, can be explained as; A and B are cations of different size and O is the anion (Zhou et al., 2018).

The B atom has 6 fold co-ordination number and the A atom have 12 fold co-ordination number, the A site cation is slightly larger than B cation. Atom B is found at the cube corner position and A is at the body center while oxygen atoms are at face-centered positions (Zhou et al., 2018) but O is the oxygen ion has the ratio of 1:1:3.

Perovskite has highly stable structure, large number of compounds, variation of properties, and various applied applications. Key role of the BO6 octahedral in ferromagnetism and Ferroelectricity. Broad formation of solid solutions lead to material optimization by structure control and phase transition engineering (Zuo and Ding, 2017). A distinctive unit cell structure of a simple perovskite compound is shown in Figs. 1–3. The perovskite structure is stable when 0.89

———————— t ———————— 1.06 (taking rO = 0.14 nm). Ideal cubic structure only observed at room temperature when t is close to 1. If A ions are small, t < 1, and tetragonal, orthorhombic and rhombohedral deformations of structure due to rotation and tilting of the BO6 octahedral are observed.

Some changes may exist in perovskite ideal cubic form which lead to the formation of orthorhombic, rhombohedral, hexagonal, and tetragonal forms. Generally to fulfill perovskite formation, two requirements should be exist those are electroneutrality and Ionic radii requirements (Shi and Jayatissa (2018)).

Other types of deformations are induced by the appearance of spontaneous polarization in ferroelectric perovskites. The perovskite structure provides the building blocks for the assembly of other important crystal structures (Huang et al., 2017) such as: Roddlesden-Popper phases (Can+1TinO3n+1), Aurivillius compounds ((Bi2O2)2+(Bim1TimO3m+1)2) and oxygen-deficient brownmillerite compounds (CaAlFeO5).

Perovskite halide construction depend on three issues: (1) the constancy of the BX6 octahedron expected by the octahedral factor m, (2) neutrality of the charges between the cations and anions, and (3) A, B and X the ionic radii are in agreement with the necessities of the Goldschmidt tolerance factor (Conings et al., 2014).

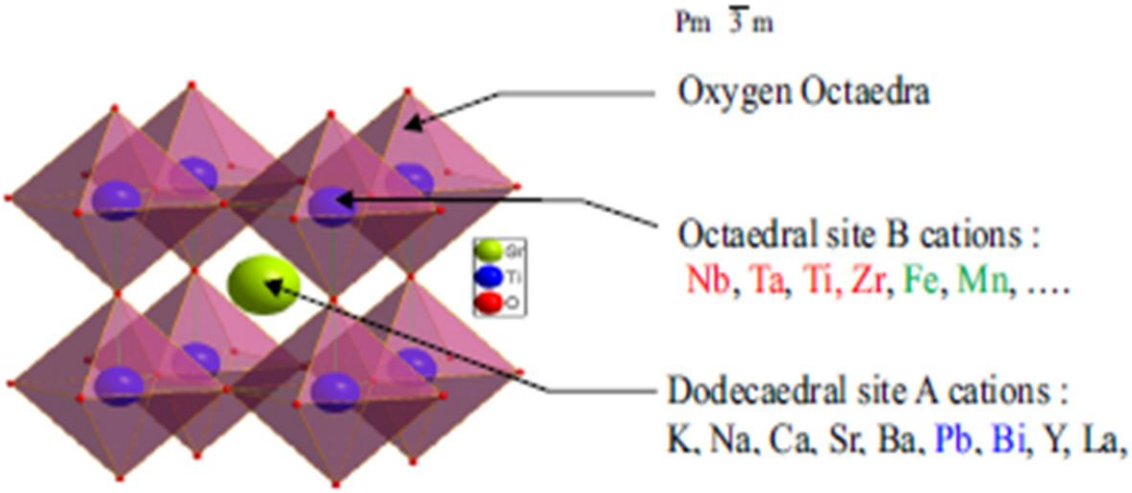

Fig. 2: Cubic perovskite SrTiO3

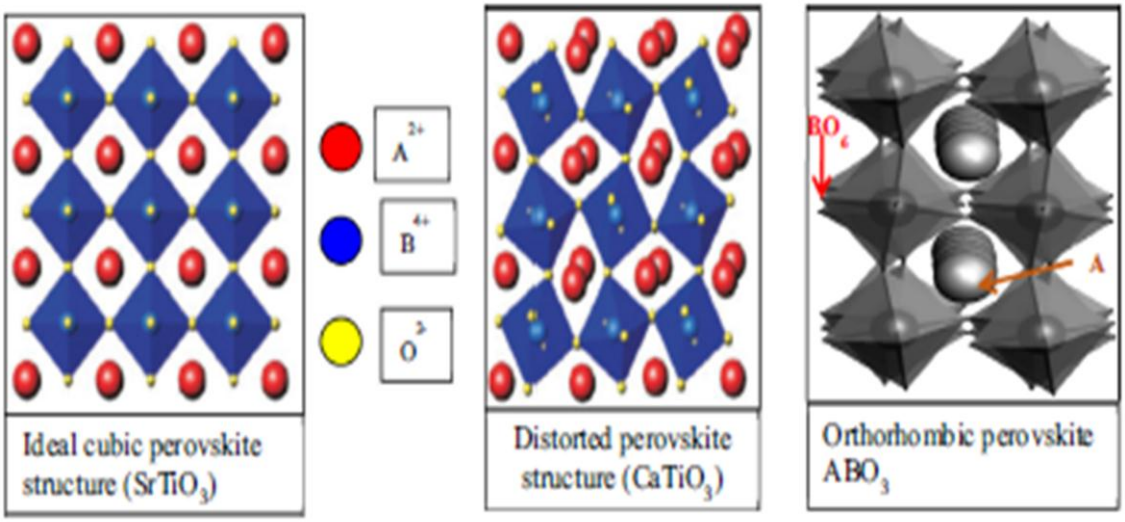

Fig. 3: The perovskite structures and deformations

2.2 CLASSIFICATION OF PEROVSKITES

A classification of the perovskite-type structures on the basis of the radii of the constituent metallic ions has been attempted by several workers (Kuzmanovski et al., 2007). Due to the flexibility of the ABO3 perovskite crystal structure in addition to its ability to accommodate a wide range of cations with different oxidation states.

The opportunity for several substitutions at the position of the cations is the main characteristic of perovskites (Dimitrovska et al., 2005) which lead to the occurrence of big groups of compounds with dissimilar cations in B position (ABxB1xO3); with different cations in A position (AxA1xBO3); and with substitution in both cation position (AxA1xBxB1xO3).

A and B cations valences are generally close to 2+ and 4+; respectively, but in some cases their valences will be 3+ for both elements only if the B3+ cation has a six coordination. The oxide phases have been mainly divided into two types (Galasso, 2013).

1. Ternary oxide ABO3 type and their solid solutions which on the basis of oxidation states can be classified into A1+B5+O3, A2+B4+O3, A3+B3+O3 and oxygen and cation deficient species (Galasso, 2013)
2. Newer complex type compounds (AB0xB00y) O3 where B0 and B00 are two different elements in different oxidation states (Bhalla et al., 2000)

and $x + y = 1$

The buckling of the (AO3)4 layers courses in the perovskite structures due to distortion or displacement of the oxygen anion array which caused by the valence variation at the A cation position (Pengfei et al., 2017). This buckling lead to distortion of the octahedra with B cations at the centers, in this case B cation must have the flexibility to tolerate this effect (Huang et al., 2016). For filling the B cation position, the transition metal elements are the most suitable candidates due to its multi valency or the special 3d and 4d electron configurations. This is the reason that transition metal oxides have perovskite-type structures and they usually have extraordinary physical properties (Niu et al., 2015).

Compounds of perovskite complex type, A ($Bx^{/}$ $By^{//}$) O_3, can be divided into four subgroups (Modeshia and Walton (2010)):

a) Compounds with oxygen deficient phases, A ($Bx^{/}$ $By^{//}$) O_{3-z}.
b) Others which contain equal amounts of the two B elements only, A ($B^{/}_{0.5}$ $B^{/}_{0.5}$) O_3
c) Those in which contain the higher valence state element are twice in value than the lower valence state element, A ($B^{/}_{0.33}$ $B^{//}_{0.67}$) O_3,
d) Those which contain the higher valence state element in twice values as much as lower valence state element, A ($B^{/}_{0.67}$ $B^{//}_{0.33}$) O_3,

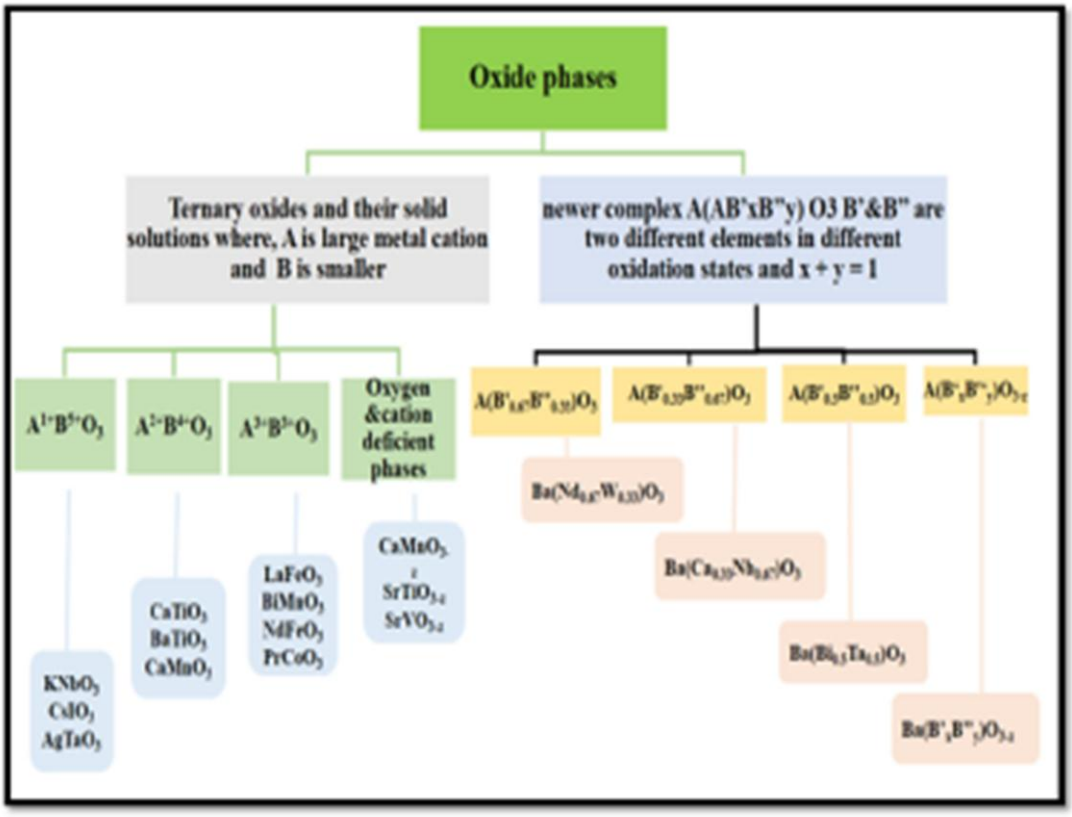

Fig. 4: Classification of perovskite structure flowchart

2.3 PROPERTIES OF PEROVSKITE SYSTEMS

Perovskite materials exhibit many interesting properties due to its characteristic chemical nature such as; their non-stoichiometry of the anions and/or cations, the valence mixture electronic structure, the distortion of the cation configuration, and the mixed valence (Kim et al., 2005).

The possibility of Perovskite to synthesizing multicomponent by partial substitution of cations in positions A and B gives rise to various complex types with peculiar properties such as; Dielectric properties, Optical properties, Ferroelectricity, Superconductivity, Piezoelectricity, Multiferroicity, Colossal magneto-resistance (CMR) and Catalytic activity (Kim et al., 2005).

2.3.1 Dielectric properties

Dielectric materials are the materials in which electro-static fields can persevere for a long time (Niu et al., 2015). It showed a great resistance to electric current channel below the action of the applied direct current voltage and diverges sharply in their simple electrical properties from conductive materials. Layers of these substances are generally inserted into capacitors to improve their performance, and the term dielectric refers to this application (Xiao et al., 2011).

Great dielectric permittivity or ferroelectric materials are of massive importance as electroceramics for engineering and electronics industry. Ferro-electricity is generally described by a soft-mode model (Hoefler et al., 2017). Several routes have been pursued to explain the dielectric and mechanical properties starting from the simple structure BaTiO3 by the solid solution system Pb (Zr,Ti)O3 to

other distinct families of materials. These routes care about the flexibility of chemical manipulation and submissiveness of the perovskites (Bhatti et al., 2016).

Relaxor ferroelectric is one of the routes, which show some effects because of the to slow reduction processes for temperatures above a glass transition (Xiao et al., 2011) such as; big dielectric constants, a marked frequency dispersion and difference in dielectric constant (Kim and Yoon, 2000).

General examples for relaxor ferroelectrics are lead lanthanum zirconate titanate (PZT) and lead magnesium niobate (PMN). Ferroelectrics can be considered as ferroelectric crystals (Zheludev, 2012) and both of its high dielectric constant and low dielectric loss make perovskites one of the best candidates for tunable microwave device applications and dynamic random access memory (DRAM) (Dongling et al., 2012).

2.3.2 OPTICAL PROPERTIES

Perovskites have provide very special class of materials with excellent optical and photoluminescence properties. Studying the optical properties of single domain crystals of BaTiO3 at various temperatures (Ohta and Hiramatsu (2018)) showed that the refractive index of the crystal was nearly a constant value (2.4 from 20_to 90 _C & reached 2.46 at 120 _C) (Zhang et al., 2017). The single crystal of BaTiO3, 0.25 mm thick was found to transmit from 0.5 l to

6 l. The optical coefficient of strontium titanate single crystals was obtained from 0.20 l to 17 l in wavelength (Xin et al., 2019).

The optical density of CaTiO3 showed absorption characteristics quite similar to those of SrTiO3 crystals with the exception that the absorptions are shifted to shorter wavelengths (Zhang et al., 2008). Both of these compounds have been considered for high temperature infrared windows. SrTiO3 is considered as an excellent material for use with optically immersed infrared detectors (Jia et al., 2003).

Some perovskites electro-optic coefficients of are nearly constant with temperature (Pinel et al., 2004). Potassium tantalite niobate (KTN) is one of the perovskite oxides which has a large room temperature electro-optic effect and wide-angle fast optical beam scanner, therefore this type is not only useful to optical communications, but also to various other products that use optical beams, such as laser application. Using of perovskite laser host materials is a great deal. Luminescent properties of all uncommon earth ions in perovskite-type oxides are highly stable and can work in various environments (Wang et al., 2008) in addition to they conceded to be the best candidate in field plasma display panel (PDP) devices and emission display (FED) because they are suitably conductive to release electric charges stored on the phosphor particle surfaces (Neeraj et al., 2004). Phosphors of rare earth ions doped perovskite type oxides (Dhahri et al., 2014) could be widely used in displays, X-ray

phosphors.

One of the environmental friendly photoluminescence (PL) is $BaZrO_3$ which emits light in the visible region and prepared easily at low cost (Di et al., 2018; Yagi, 2009). The property of PL makes it promising for applications such as; scintillators, solid state lightning, field emission displays, green photocatalyst and plasma displays (Sayyadi-Shahraki et al., 2017).

2.3.3 FERROELECTRICITY

Ferroelectricity is the phenomenon that occurs when an external electric field is applied to some materials leading to a spontaneous electric polarization (Retot et al., 2008; Cross, 2011). The discovery of ferroelectricity in perovskite-based materials and other barium titanate ($BaTiO_3$) opened up new different application for ferroelectric materials, leading to significant interest in other types of ferroelectrics (Morris, 2018; López-Juárez et al., 2011).

The ferroelectric materials have dielectric constant twice larger in magnitude than those in ordinary dielectric. $BaTiO_3$ is a well-known ferroelectric material with relative dielectric constant, its crystal at room temperature, exhibits no net polarization, in the absence of an external field, even though the dipoles of adjacent unit cells are aligned (Xu, 2011).

Ferroelectric property is used to several purposes such as; in ultrasound imaging

devices, fire sensors, infrared cameras, vibration sensors, tunable capacitors, memory devices, RAM and RFID cards, input devices in ultrasound imaging, and a. make sensors, capacitors, memory devices, etc. (Raghavan, 2015).

2.3.4 SUPERCONDUCTIVITY

Certain materials once cooled under a specific serious temperature exhibited zero electrical resistance and expulsion of magnetic flux fields this phenomenon called Superconductivity (Kittel, 2005). The oxide perovskites structure type provides an excellent structural framework due to the existence of superconductivity.

Perovskites which have Cu act as high-temperature superconductors. The first reported example of superconducting perovskites is La-Ba-Cu-O perovskite and there are many more (Mourachkine, 2004). Perovskite oxides now eclipsed the use of Intermetallic compounds as source of many superconducting materials such

as; cesium tungsten bronzes and Sodium, potassium, rubidium (Cava, 2008).

Type 2 group Superconducting ‘‘perovskites” metal-oxide ceramics are those compounds which have specific ratio of 2 metal atoms to every 3 oxygen atoms (Morita et al., 2006). This type of superconductors is contained of alloys and metallic compounds (excluding for niobium, vanadium, and technetium), recently they achieve higher transition temperature than Type 1 superconductors

(Ishihara (2009)).

2.3.5 PIEZOELECTRICITY

Some materials have the capacity to produce an electric charge in reaction to applied mechanical stress is known as Piezoelectricity (Wang et al. 2004). Therefore, if definite crystals were subjected to mechanical strain, they became polarized at a degree which is proportional to the applied strain (Wang et al., 2006). On the other hand, they have some changed when they were exposed to an electric field which is known as the inverse piezoelectric effect (Brockmann, 2009).

There is a difference between piezoelectric and ferroelectric materials, in the fires materials it requires some external impetus while in the second there is spontaneous alignment of electric dipoles by their mutual interaction. Therefore, all piezoelectric are not ferroelectric but all ferroelectrics are piezoelectric.

Some synthetic piezoelectric materials are the piezoelectric ceramics with the perovskite crystal structure (Aksel et al., 2011) having a general formula of A2+B4+O2_3. Also there are naturallyoccurring piezoelectric materials; quartz, cane sugar, collagen, topaz, rochelle salt, tendon, etc.

Perovskites materials Piezoelectricity property have many valuable scientific

application (Ye, 2008) such as; Cigarette lighter, Sensors, Microphones, High voltage and power source, Pick-ups, Pressure sensor, Force sensor, Strain gauge, Actuators, Piezoelectric motors, Piezoelectric motors, Nano-positioning in AFM, STM, Acuosto-optic modulators, Loudspeaker, Valves, Energy harvesting, AC voltage multiplier (Kleckers, 2013).

2.3.6 MULTIFERROICITY

Multiferroics include special class of materials showing concurrent ferroelectric, ferromagnetic, and ferroelastic ordering. The specialty of these materials localized in their ability to simultaneous utilization of their magnetization and polarization states, a potential which make them excellent candidates for memory devices and sensors (Spaldin et al., 2010; Ramesh and Spaldin, 2007). Many multiferroics are transition metal oxides with perovskite crystal structure, and include rare-earth manganite and ferrites (Wang et al., 2010). These materials shows multiferroicity even at room temperature (Kézsmárki et al., 2011). Bismuth ferrite, a rhombohedrally distorted perovskite (compounds with multiferroics property) possesses both anti-ferromagnetic and ferroelectric order for a widespread temperature range which is greatly above room temperature (Singh et al., 2011). Most of the ferromagnetic materials are generally metals and they must be an insulator because the absence of insulators limits the

simultaneous occurrence of ferromagnetic and ferroelectric ordering (Ghosh et al., 2019). The important requirement for ferroelectricity is a structural distortion from the high symmetry phase that removes the center of inversion and allows an electric polarization (Fig. 6) (Zverev et al., 2014). It has been found that even in the absence of any structural distortion, magnetic spin ordering can produce ferroelectricity. Multiferroics have great technological potential importance due to the co-occurrence of magnetic order and ferroelectric polarization joint in a single-phase material (Eerenstein et al., 2006). Multiferroic materials open promising opportunities for spintronics devices and designing novel microelectronic (Bai et al., 2005). It has been found that even in the absence of any structural distortion, magnetic spin ordering can produce ferroelectricity. Multiferroicity, a co-occurrence of natural ferroelectric and ferromagnetic moments, is an uncommon phenomenon due to the minor number of asymmetry magnetic point groups that permit an unplanned polarization (Johnson and Radaelli, 2014).

Multiferroic materials classified into Type I & type II Multiferroic. Type I includes the structures with nonpolar-to-polar phase transition which responsible about the breaking of reversal equilibrium leading to ferroelectricity at high temperatures. While in type II the primary order parameter is the staggered (antiferromagnetic) magnetization (Liu et al., 2011). In addition, if the magnetic ordering goes below a given temperature, it lowers both

magnetostructural coupling to the crystal structure (this gives rise to an electrically polar state) and the symmetry group from polar magnetic phase to a nonpolar parent phase making wrong ferroelectricity therefore ferroelectric order and magnetic factors are closely joined (Francis et al., 2016).

2.3.7 COLOSSAL MAGNETO RESISTANCE (CMR)

Colossal magneto resistance (CMR) is a property of particular materials (mostly manganese-based perovskite oxides) that allows them to change their electrical resistance in the presence of a magnetic field (Lu et al., 2004). The discovery of this property (CMR) affect the divalent alkaline-earth ion doped perovskite manganite RE1_xAExMnO3, where AE represents divalent alkaline earth ions (Ca, Sr, Ba) and RE is trivalent rare-earth (La, Pr, Sm, etc.) (Garg et al., 2009). Magnetic phases are observed depending on the orbital occupancy of the manganese ions and the associated orbital order, different. In these compounds, ordering temperatures of similar magnitude for both degrees of freedom because their orbitals and spins are strongly coupled (Feroze et al., 2017).

On the other hand, magnetic frustration, low dimensionality, and quantum effects lead to very peculiar phase graphs with or without magnetic long range order. In unfulfilled lattices the degeneracy of the magnetic zero state can be frequently lifted by second order energy scale or quantum fluctuations (Tokura, 2006). Generally, CMR effect is closely related to its manganites which are

correlated electron systems with interplay among the lattice spin, Jahn-Taller effect, charge & orbital degrees of freedom, electronic phase separation, charge ordering, etc. (Rojas-Cervantes and Castillejos, 2019).

2.3.8 CATALYTIC ACTIVITY

Perovskites displayed exceptional catalytic action and great chemical stability therefor it includes in the catalysis of changed reactions. Also, it can be defined as an oxidation or oxygenactivated catalyst and as a model of active sites (Roni, 2018). The perovskite structure showed high catalytic activity in addition there stability allowed the preparation of several compounds from elements with uncommon valence statuses or a great extent of oxygen lack (Roni, 2018). They also can act as motor exhaust gas catalyst, cleaning catalyst, and intelligent automobile catalyst for various catalytic environmental reactions. Some Perovskite types (containing Cu, Co, Mn, or Fe) showed catalytic action to the straight decay of NO at high temperature due to the occurrence of oxygen deficiency and the simple removal of the surface oxygen in the a shape of a reaction product (Nishihata et al., 2005). Perovskite revealed a great effect as a vehicle catalyst; intelligent catalyst, removal of CO &NO, effective catalyst and Not combusted hydrocarbons. It can show redox properties to reserve unlimited scattering state (Singh et al., 2007) and when oxidation occurs fine metal bits of Pd will form with radius of 1–3 nm. This lead to partial replacement of Pd into

and sedimentation from the structure of the perovskite under decreasing and oxidizing states showing a great scattering state of Pd. This cycle improved the long-standing reliability of Pd through the pollutants elimination from the exhaust gas. The great stability of the perovskite structure and the unlimited spreading state of Pd were the cause of calling it as intelligent catalyst (Wang et al., 2014) (see Table 1).

Table 2.1: Properties of Perovskite Oxides

Typical Properties	Typical Compound
Ferromagnetic	BaTiO3, PdTiO3
Piezoelectricity	Pb(Zr, Ti)O3, (Bi, Na)TiO3
Superconductivity	La0.9Sr0.1CuO3, YBa2Cu3O7, HgBa2Ca2Cu2O8
Ion conductivity	La(Ca)AlO3 BaZrO3, CaTiO3, SrZrO3, BaCeO3, La(Sr)Ga(Mg)O3,
Magnetic property	LaMnO3, LaFeO3, La2NiMnO6
Catalytic property	LaCoO3, LaMnO3, BaCuO3
Electrode	La0.6Sr0.4CoO3, La0.8Ca0.2MnO3
Piezoelectricity	Pb(Zr, Ti)O3, (Bi, Na)TiO3

2.4 APPLICATIONS OF PEROVSKITES

Perovskite oxides types are have wide applications due to its stable structure, large number of compounds, variety of properties (Deka et al., 2014). Inorganic perovskite type oxides are attractive nanomaterial for varied applications due to its large number of compounds, very stable structure, variety of properties and several practical applications. Some of these compounds nanomaterial are wildly applied in catalysis of many chemical engendering fields. The activity of these oxides as catalyst is better than any other transition metals and precious metal oxides. Depending on Perovskite oxides distinct variety of properties they became useful for various applications such as; Thin film capacitors, Non-volatile memories, Photo-electrochemical cells, Recording applications, Read heads in hard disks, Spintronics devices, Laser applications, For windows to protect from high temperature infrared radiations, High temperature heating applications, Thermal barrier coatings, Frequency filters for wireless communications, Non-volatile memories, Sensors, actuators and transducers, Drug delivery, Catalysts in modern chemical industry, Ultra-sonic imaging, ultrasonic & underwater devices (Ottochian et al., 2014). Some more important applications of different perovskite structured are listed in Table 2.

Recently, they utilized in electrochemical sensing of alcohols, acetone, glucose, gases, amino acids, H2O2, sensitivity, excellent reproducibility, unique long-

term stability, anti-interference ability and neurotransmitters exhibiting good selectivity, etc.. In addition, some perovskites are worthy applicants for the development of effective anodic catalysts for direct fuel cells viewing high catalytic performance (Kumar and Chand, 2018). Some details of the application are summarized in the following.

2.4.1 SENSORS AND BIOSENSORS

GAS SENSORS

There are a sum of necessities that the resources used as gas devices must content such as hydrothermal constancy, good similarity with the target gases, suitable electronic structure, resistance to poisoning, and alteration with existing skills (Christen and Eres, 2008).

Perovskite oxides used as gas sensors like semiconductors, LaFeO3 and SrTiO3. They are interesting materials as gas sensors for their ideal band gap, thermal stability, and size difference between the cations of B-- and A sites. Perovskites materials which contain cobaltates, titanates, and ferrites were applied as gas sensors for spotting CO, NO2, methanol, ethanol, and hydrocarbons (Taylor et al., 2019).

GLUCOSE SENSOR

It is important to determined H2O2 and glucose in numerous fields in our live

such as in food, pharmaceutical products and clinic. H2O2 is oxidizing agents in many neutrinos and industries. Glucose also is the basic metabolite in many of the living organisms and in clinical check of diabetes mellitus, and universal healthiness problem. Therefore it is important to have excellent sensitive biosensors for determination both H2O2 and glucose (Ottochian et al., 2014).

Although there are different types of enzymatic work as glucose sensors but these enzyme lack the stability due to its basic nature in addition its action was greatly affected by poisonous chemicals, temperature, humidity, etc. consequence, there must be searching for stable, sensitive, simple, and selective non-enzymatic glucose sensor such as inorganic perovskite oxides (Jia et al., 2015).

These sensors have perfect electrocatalytic activity toward glucose and H2O2 oxidation in alkaline medium due to the occurrence of huge amount of active sites in the modifier.

NEUROTRANSMITTERS SENSOR

In the mammalian central nervous system, dopamine (DA) is an essential catecholamine neurotransmitter. The deficiency of this transmitter lead to Parkinson's disease; therefore, its detection is very important but there are very big problem in detection of DA which is the interference of ascorbic acid (AA) and uric acid (UA) with its detection (Jia et al., 2015). Therefore, it is very

important to find sensitively and selectively detector to DA even in presence of high concentration of AA and UA.

After electrode modified of SrPdO3 (CpE/SrPdO3) it became very good electrochemical DA sensor in living liquids with exclusive long-term constancy and low discovery limit even in the occurrence of high level of AA and UA, it also can sense DA in human urine samples with full selectivity recovery, precision, accuracy, and detection limit (Zhang et al., 2013).

2.4.2 SOLID OXIDE FUEL CELLS

Fuel cells are used as substitutes to ignition engines due to their possibility to reduce of the environmental pollution. They uses specific type of chemical compound as energy source which transfer to electrical energy like battery. Fuel cells are more acceptable for use due to their effectiveness, spread nature, zero noise pollution, low emissions and its use in future hydrogen fuel economy.
There are numerous categories of fuel cells but solid oxide fuel cell are the greatest common samples of fuel cells (El-Ads et al., 2015).

Due to the variances of electrical conductive characteristics of perovskites, they are selected as an active component in SOFC (Wang et al., 2012) because they

exhibited its properties of electrical conductivity which is comparable to that of metals with high ionic conductivity, and perfect mixed ionic and electronic conductivity (Atta et al., 2013).

2.4.3 CATALYST

Perovskite oxides are used universally as catalyst in new chemical manufacturing, showing suitable solid-state, surface, and morphological properties (Thirumalairajan et al., 2013). Several perovskites oxides proved to have excellent catalytic activity to different reactions like hydrogen evolution, reduction reactions, and oxygen evolution (Lianghao et al., 2015).

2.4.4 SOLAR CELLS

One of the green sources of energy is solar energy because it can be used in replace of the fossil fuels energy. Solar radiation can be transform to electrical energy in a suitable way building numerous uses for solar energy. It can be perfectly changed into electricity using photovoltaic solar cells which built on silicon. The disadvantage of silicon built solar cell is its high price of electricity produced from it, so develop solar cell with low cost is needed (Wang et al., 2012; Li et al., 2016).

Solar cells created on organic/ inorganic solid-state methyl ammonium lead

halide hybrid perovskite are in used because it presented better points such 20% lower cost than that of traditional silicon solar cells in addition to the availability of the raw materials (Jin et al., 2013). Perovskite showed outstanding essential properties for photovoltaic applications like suitable band gap, excellent stability, long hole-electron diffusion length, high absorption coefficient, high carrier mobility & transport, low temperature of processing, charge carriers with small effective mass and easy processing steps (Bao et al., 2015).

Table 2.2: Some Important Applications of Perovskite structures and their properties

Reference Compound	Properties	Existing and potential applications	Notes
BaTiO3	Ferroelectricity, high dielectric constant, piezoelectricity	Multilayer ceramic capacitors (MLCCs), embedded capacitance, PTCR resistors,	Most widely used dielectric ceramic TC = 125 _C
(Ba,Sr)TiO3	Non-linear dielectric properties	Tunable microwave devices	Used in the paraelectric state
Pb(Zr,Ti)O3	Piezoelectricity, Ferroelectricity	Piezoelectric transducers and actuators, ferroelectric memories (FERAMs)	PZT: most successful piezoelectric material
Bi4Ti3O12	Ferroelectric with high Curie temperature	High-temperature actuators, FeRAMs	Aurivillius compound
(K0.5Na0.5)NbO3, Na0.5Bi0.5TiO3)	Ferroelectricity, piezoelectricity	Lead-free piezoceramics	Performances not yet comparable to PZT
(Pb,La)(Ti,Zr)O3	Transparent ferroelectric	Optoelectronic devices	First transparent ferroelectric ceramic

CHAPTER THREE

METHODOLOGY

3.1 DENSITY FUNCTIONAL THEORY (DFT)

Density-functional theory (DFT) is a computational quantum mechanical modeling tool used in physics, chemistry, and materials science to examine the electronic structure (or nuclear structure) (mostly the ground state) of many-body systems, including atoms, molecules, and condensed phases. The properties of a many-electron system can be calculated using this theory by using functional, which are functions of another function. These are functional of the spatially dependent electron density in the case of DFT. It is one of the most widely used and versatile techniques in condensed-matter physics, computational physics, and computational chemistry. it is one of the most popular and successful quantum mechanical approaches to matter. DFT has been very popular for calculations in solid-state physics since the 1970s. It is nowadays routinely applied for calculating, e.g. the binding energy of molecules in chemistry and the band structure (Klause Capelle 2006) of solids in physics. First applications relevant for fields traditionally considered more distant from quantum mechanics, such as biology and mineralogy are beginning to appear. Superconductivity, atoms in the focus of strong laser

pulses, relativistic effects in heavy elements and in atomic nuclei, classical liquids, and magnetic properties of alloys have all been studied with DFT. DFT owes this versatility to the generality of its :fundamental concepts and the flexibility one has in implementing them. Despite its flexibility and breadth, DFT is founded on a rather rigid conceptual foundation.

To obtain a sense of what density-functional theory is all about, it's helpful to go back to elementary quantum mechanics. We taught in quantum mechanics that all information we could possibly have about a given system is stored in the system's wave function. The nuclear degree• of freedom (e.g., the crystal lattice in a solid) appears simply as a potential; V(r) acting on the electrons so that the wave function is only dependent on the electronic coordinates. This wave function is derived non-relativistically using Schrodinger's equation, which for a single electron travelling in a potential V(r) reads:

$$\left[\frac{-h}{2m}\nabla + v(r)\right]\varphi(r) = \epsilon\varphi(r) \qquad \textbf{(2.1)}$$

If there is more than one electron (i.e. one has a many-body problem), the Schrodinger equation becomes

$$\left[\sum_i^N \left(\frac{-h}{2m}\nabla + v(ri)\right) + \sum U(rr)\right]\varphi(r,r) = \epsilon\varphi(r_i, r_j \ldots . r_N) \qquad \textbf{(2.2)}$$

Where N is the number of electrons and $U(r_i r_j)$, interaction. For a coulomb system one has

$$\widehat{\boldsymbol{U}} = \sum \boldsymbol{U_i}(\boldsymbol{r_i r_j}) = \sum_{r_i}^{2} \frac{\boldsymbol{q}}{\boldsymbol{r-I}} \quad \textbf{(2.3)}$$

Whether our system is an atom, a molecule, or a solid thus depends only on thepotential $V(r_i)$. For an atom.

$$\widehat{\boldsymbol{V}} = \sum \boldsymbol{v}(\boldsymbol{r}) = \sum \frac{\boldsymbol{Qq}}{\boldsymbol{r-R}} \quad \textbf{(2.4)}$$

Where Q is the nuclear charge and R is the nuclear position. When dealing with a single atom, R is usually taken to be the zero of the coordinate system. For a molecule ora solid one has;

$$\widehat{\boldsymbol{V}} = \sum \boldsymbol{v}(\boldsymbol{r_i}) = \frac{\boldsymbol{Qq}}{\sum \boldsymbol{ir-R_{ik}}} \quad \textbf{(2.5)}$$

Where the sum on k extends over all nuclei in the system, each with charge and positionR_k, One specifies the system by choosing $V_{(r)}$, plugs it into Schrodinger's equation, solves that equation for the wave function, and then calculates observables by taking expectation values of operators with this wave function. One among the observables that are calculated in this way is the particle density.

$$\boldsymbol{n(r) = N \int d^3 r_2 \int d^3 r_3 \ldots\ldots \int d^3 r_N \varphi(r_1, r_2, \ldots r_N)\varphi(r_1, r_2, \ldots r_N)} \quad \textbf{(2.6)}$$

Many powerful methods for solving Schrodinger's equation have been developed during decade of struggling with the many-body problem. In physics,

for example, one has diagrammatic perturbation theory (based on Feynman diagrams and Green's functions), while in Chemistry one often uses configuration interaction (CI) methods, which are based on systematic expansion in Slater determinants. A host of more special techniques also exists. The problem with these methods is the great demand they place on one's computational resources: it is simply impossible to apply them efficiently to large and complex systems. It is here where DFT provides a viable alternative less accurate perhaps, but much more versatile. The density-functional approach can be summarized by the sequence

$$\boldsymbol{n(r) = \varphi(r, \ldots . r_N) = v(r)} \qquad \textbf{(2.7)}$$

i.e. knowledge of n(r) implies knowledge of the wave function and the potential and hence of all other observables.

3.2 PSEUDOPOTENTIALS ANDAPPLICATIONS

A pseudo potential or effective potential is a physics approximation used to simplify the description of complex systems. Atomic physics and neutron scattering are two examples of applications. Hans Hellmann invented the pseudo potential approximation in 1934. The pseudo potential is an attempt to replace the complicated effects of an atom's and its nucleus's motion of core (i.e. non-valence) electrons with an effective potential, or pseudo potential, so that the Schrödinger equation contains a modified effective potential term instead of

the Columbic potential term for core electrons normally found in the Schrödinger equation. The pseudo potential is an effective potential constructed to replace the atomic all-electron potential (full-potential) such that core states are eliminated and the valence electrons are described by pseudo-wavefunctions with significantly fewer nodes. This allows the pseudo-wave functions to be described with far fewer Fourier modes, thus making plane-wave basis sets practical to use. In this approach usually only the chemically active valence electrons are dealt with explicitly, while the core electrons are 'frozen', being considered together with the nuclei as rigid non-polarizable ion cores. It is possible to self-consistently update the pseudopotential with the chemical environment that it is embedded in, having the effect of relaxing the frozen core approximation, although this is rarely done. In codes using local basis functions, like Gaussian, often effective core potentials are used that only freeze the core electrons.

One of the main advantages of using a plane wave basis set is that its accuracy can be easily controlled. This is related to the fact that, when using such a basis set, we are making no assumptions about the final shape of the orbitals, other than that there is some scale below which they become smoothly varying (Stewart Clark, 2012). However, this also leads to a major disadvantage of using a plane wave basis set, which is that the size of the basis set required for a given system is often far

larger than would be required with a localized basis set. This is because, in condensed matter systems, the orbitals tend to oscillate very rapidly in the vicinity of atomic nuclei, and are much more smoothly varying elsewhere. In order to describe this rapid oscillation we must set a very large cut-off energy, so that we include plane waves with very short wavelengths. But, since most of the space in the cell does not contain rapidly oscillating orbitals, most of the computational expenses associated with all these plane waves effectively goes to waste. A localized basis set can be tailored such that the basic functions themselves are rapidly oscillating in the vicinity of atomic nuclei and more smoothly oscillating elsewhere, so that the total number of basic functions required for the system is far smaller.

The use of pseudopotential, in conjunction with plane waves, can dramatically reducethemagnitudeofthisproblem.Tounderstandwhatpseudopotentialdoes, we note the following two facts about orbitals in condensed matter system.

i. Lower energy orbitals can often be considered to represent core electrons. These are electrons that are well localized around an atomic nucleus and whose properties do not change significantly

with the atom's chemical environment.

ii. Orbitals representing electrons that are not core electrons oscillate very rapidly in the vicinity of atomic nuclei, but most of this oscillation can be put down to the fact that they have to be orthogonal to the core electrons. A pseudopotential essentially changes part of what the outer, or valence, electrons "see." The core electrons, and the potential due to the bare nuclear charge, are replaced by a fictitious potential that is defined such that the behaviour of the valence electrons is not affected outside of some cut-off radius from the nucleus. So long as this radius is not so large that it overlaps regions of space that are involved in chemical bonding, the pseudopotential approximation should not significantly alter the inter- atomic interactions that govern the behaviour of condensed matter.

Using pseudopotential seduces the computational cost of a calculation in three ways;

(a) By effectively removing core electrons from the calculation, the number of Kohn-Sham orbitals is reduced. This reduces the memory required to store the orbitals, the time required to evaluate orbital-dependent quantities, and the time required to orthonormalise a set of orbitals.

(b) Because there are no core-electrons to which valence electrons must be

orthogonal, there is less oscillation of the corresponding orbitals in the vicinity of the nucleus. This means that a lower cut-off energy can be used to represent the orbitals, resulting in lower memory requirements and greater speed. This lowering of the cut-off energy is typically a few orders of magnitude resulting in massive gains inefficiency.

(c) Because the pseudopotential is not uniquely defined for a particular element, we can optimize the shape of the potential so as to give as low a required cut-off energy as possible. Again, this reduces memory and increases speed. Because we only explicitly treat the valence electrons in a calculation when using pseudopotentials, we tend to think of the system as being made of electrons and ions rather that electrons and nuclei.

3.2.1 Quantum ESPRESSO

Quantum ESPRESSO is a free, open-source software suite for ab initio quantum chemistry methods of electronic-structure calculation and materials modeling. Density Functional Theory, plane wave basis sets, and pseudopotentials serve as its foundation (both norm-conserving and ultra-soft). The abbreviation ESPRESSO stands for Open Source Package for Research in Electronic Structure, Simulation, and

Optimization. The PWscf component provides the core plane wave DFT functions of QE; PWscf was previously an independent project. PWscf (Plane-Wave Self-Consistent Field) is a program that uses plane wave basis sets and pseudopotentials to calculate electronic structure in density functional theory and density functional perturbation theory. The software is distributed under the terms of the GNU General Public License.

Quantum ESPRESSO is an open initiative, of the CNR-IOM DEMOCRITOS National Simulation Center in Trieste (Italy) and its partners, in collaboration with different centers worldwide such as MIT, Princeton University, the University of Minnesota or the Ecole Polytechnique Federale de Lausanne. The project is coordinated by the QUANTUM ESPRESSO foundation which is formed by many research centers and groups all over the world. The first version called pw. l.0.0, was released on 15-06-2001.

The program, written mainly in fortran-90 with some parts in C or in Fortran-77, was built out of the merging and re-engineering of different independently- developed core packages, plus a set of packages, designed to be inter-operable with the core components, which allow the performance of more advanced tasks.

Basic packages include Pwscf (Corso, Andrea Dal, 1996). Which solves

the self- consistent Kohn and Sham equations, obtained for a periodic solid, CP to carryout Car-Parrinello molecular dynamics, and PostProc, which allows data analysis and plotting. Regarding the additional packages, is noteworthy to point out atomic for the pseudopotential generation, Phonon package, which implements density- functional perturbation theory (DFPT) for the calculation of second- and third-order derivatives of the energy with respect to atomic displacements and NEB: for the calculation of reaction pathways and energy barriers.

& CONTROL

Calculation = 'scf ',

Outdir = './tmp ',

Pseudo _dir = 'dr/to/pseudopotentials ',

Prefix = 'pwscf/

& SYSTEM

ibrav =2,

celldm(l) =7.6525971195,

nat =1,

ntyp =1,

ecutwfc =30

ecutrho =120,

occupations = 'smearing',

degauss =0.005,

smearing = 'marzari~vunderbill

& ELECTRONS

conv_thr = Id-06,

mixingjbeta = 0.7d0,

& ATOMIC, SPECIES

A126.98150 Al.pz-n-rrkjusjpsl. 0.1.UPF

ATOMIC_POSITIONS*Crystal*

Al 0.000000000 0.000000000 0.000000000

K-POINTS automatic

888000

2.4.2 Post Processing

Stafano Baroni, Stefano de Gironcoli, Andrea Dal Corson (SISSA), Paolo Giannozzi (Univ. Udine), and many others created the post processing software. After converting the self-consistent calculation, we employ various tiny calculations such as band charting, density of states (DOS), and so on. The following are the key post processing scripts that extract the given data/files from the PWSCF computations and do further calculations:

- **P.W.X:** We use this command to ran the input files of scf and nscf calculations of energy and wave functions at each and every k-points, which extracts the output files for the energy calculation at every k-points.
- **Bands. x:** This extracts the files form pwscf calculation and records its Eigen Values at different k-points with corresponding energies values ready for their processing. The code bands.x also performs the symmetry analysis of the band structure.
- **Plotband. x:** The output file of bands. x is directly read and converted to plottable format by auxiliary code plotband. x. The value of k-points must becorrectly put in a sequence, otherwise unpredictable plots may results if k- points are not in sequence along lines or if two consecutive points are same. Thus proper choice of sequence of k-points is important.
- **Dos. X:** This code helps us to calculate the electronic density of states at different k-poiints.
- **projwfc. x:** This code calculates projections of wave functions over atomic orbitals. It gives the contributions of the atomic orbitals s,p,d,f.

3.2.3 Band Structure

In the first principle, electronic structure calculation of crystals, the electronic band structure is one of the most widely applied analytical tools especially within the Kohn-Sham framework of density functional theory. It provides the electronic levels in (ideal) crystal structures, which are characterized by a Block vector K and a band index n. Here the Block Vector is an element of the reciprocal space (in units '/length) and typically restricted to the first Brillouin Zone (Andreas Wacker, 2010). The band structure of solid are helpful to determine different electronic properties of solid. It contains the basic ingredients to almost all the crystal properties. Since the atoms in a solid are closely packed the interaction between them perturbed the initial atomic levels when a large number of atoms are brought together. Electrons in the orbitals are filled up according to Pauli's Exclusion Principle i.e. no two electron can occupy the same energy state. A bands constitutes a sort of energy continuum, in which separate level due to individual atoms cannot be identified in the process of inter atomic interaction, the inner shell electron stated are the least affected whereas the valence electron, which are closest to neighboring ions, are the most affected. The effect of bringing one atom closer to the other is to split a single sharp level. The

bands structure of solids are helpful in determining different electronic and optical properties of the solid. According to Band theory, the measure of band gap determines the types of the solid. The band structure are calculated by pseudo

potential and plane wave basis set method within the Density Functional Theory (DFT), treating exchange correlation functional with Generalized Gradient Approximation (GGA) in the form of Predew Berke-Erznd of (PBE) functional.

3.2.4 DENSITY OF STATES (DOS)

The Density of States (DOS) is defined as the number of states per unit energy range available for the particles to be occupied (Walter, 1989). In other words, the density of states refers to the number of quantum states per unit energy range and it indicates how density packed quantum states in a particular system. In solid state and condense matter physics, the density7 of states is of immense important as it can be used to calculate the various parameters that give the insight of the different electronic, magnetic and transport properties. For example, specific heat and paramagnetic susceptibility of a substance, mobility of charge carriers, diffusion properties and so on can be readily computed with the knowledge of density of states (DOS). Moreover, the density of states

provides numerical information on the states that are available at each energy level. The value of zero density of states indicates that there are no available states for occupation in an energetic level.

The density of states are calculated by pseudopotential and plane have basis set method within the Density Functional Theory (DFT), treating Exchange- Correlation Functional with generalized gradient approximation (GGA) in the form of Predew Berke-Erznd of (PBE) functional.

3.3 COMPUTATIONAL DETAILS

3.3.1 CONVERGENCE TESTS (OPTIMIZATION)

We used self-consistent field (SCF) computations to find basic parameters such as kinetic energy cut-off for the plane wave basis and k-points grid by evaluating total energy convergence with these parameters individually and computing lattice parameters through energy reduction.

KINETIC ENERGY CUTOFF (ecutwfc)

The kinetic energy cut-off, ecutwfc (in Ry) determines the size of the plane- wave (PW) basis set used to expand wave functions (i.e Kohn-shan orbitals). The value of the kinetic energy cut-off corresponds to the neighbouring interactions in the periodic system. If we take this cutoff

energy large, we include long range interactions and the results will be more accurate, but this takes more computing resources. If we take this energy small, the results could be inaccurate though computationally cheap. Therefore, we have to take optimum value of this cut-off energy.

PROCEDURES:

1. Change the value of ecutwfcin ,scf.in(e.g si.scf.in), input file to 10, 15, 20, 25, 30, 35, 40,...
2. Run pw.x again and again, noting the final energy.
3. Grep to edit the energies.
4. Complete the data in file si.etot_vs_ecut
5. Plot file si_etot_vs_ecut

For instance

$ gnuplot (then press enter)

Gnuplot> plot ‘si_etot_vs_ecut‘ using 1:2 with lines.

CELL DIMENSION (LATTICE PARAMETER)

The lattice constant is a property of the crystal lattice, which is a periodic arrangement of atoms in three dimensions, and not a property of atoms. The length of periodicity of the lattice repeats itself is essentially the lattice constant; for most crystals, the lattice constant is a few angstroms.

PROCEDURES:

1. Edit the celldm in the &SYSTEM structure
2. Increase and decrease the value of lattice constant by adding 0.1 downward and subtracting 0.1 upward.
3. Run pw.x for values
4. Grepcelldm
5. VIM to filter.

   |qe~6.2.1/bin/ev.x (press enter)

   Lattice parameter or volume are in (au, ang) >ang

   Enter type of equation of state:

   1= birch 1, 2= birch2, 3=keane, 4= mumaghan>4

   Input file >celldm

   Output file >celldm.out

   To plot graph

   Gnuplot (press enter)

   Gnuplot> p ‘celldm’ u 1:2 wl

K-POINTS GRID

A sufficiently dense grid of k-points is needed in order to account for periodicity. In order to perform the Brillouin zone interaction in discrete scheme, it is essential to have a large number of grid points. But in

practice, due to limitations of computational resources, we optimize the number of k-points grids. By calculating total energy versus k-point grids. The rectangular grid of points of dimensions k x k X k, spaced evenly throughout the Brillouin zone is called k- points grid.

PROCEDURES:

1. Edit ,scf.in(set ecutwfc back to optimized value), modifying the k-points card to use

   K points automatic

   nkl nk2 nk3
2. Run pw.x complete entries for each k points.
3. Grep
4. VIM to filter.
5. The plot the graph using the following syntax:

   $ gnuplot... press enter

   Gnuplot> plot ‘si.etot_vs_nks’ using 1:3 with lines.

3.3.2 BAND STRUCTURE PROCEDURES:

1. Open a new folder name it ‘Band’
2. Copy the following files into the folder and edit all
   - Scf.in
   - nscf.in

- Band.in

3. Open terminal/cd ...

   Cd /element/Band

Start with scf.in

nscf.in

band.in

code to compute band structure calculation

~/espresso-4.3.2/bin/pw.x<scf.in>scf.out

~/espresso-4.3.2/bin/ pw.x<nscf.in>nscf.out

~/espresso~4.3.2/bin/ bands. x<band.in>band, out

To plot graph:

~/espresso-4.3.2/bin/ Plotband.x (press return)

Input file: > Sibands.dat (press enter)

Range : -0.000 413.150ev Emin, Emax> 0.0,413 (press enter)

Output file (xmgr) > Si.Xmgr (press enter)

Output file (ps) > Si.ps (press enter)

E Fermi > 0.00 (press enter)

Delta Fe, reference E (for tics) 50,0

3.3.3 DENSITY OF STATES(DOS)

How to calculate for DOS:

1. Open a new folder, name it “DOS”

2. Copy the following files into it the folder and edit all

- Scf.in
- nscf.in
- dos.in
- pdos.in

note: all files were edited with respect to material name and scf.in

3. open terminal / cd... cd space /element/Dos

start with

a) scf.in--* pw.x<si.scf.in>si.$cf.out

b) nscf~>pw.x<si.nscf. in>si .nscf. out

c) dos.in —>dos.x<si.dos.in>si.dos.out

d) pdos ->projwfc.x<si.pdos.in>si.pdos.out

3.4 POST PROCESSING

The package called post processing was originally developed by Stefano Baroni. Stefano de Gironcoli, Andrea Dal Corso, and many others. After the self-consistent calculation has been converged. They are number of auxiliary codes performing small calculations such as plotting of band, density of states (DOS) etc. The main post processing codes which extract the specified data/files from PWscf calculations and perform further calculations are as follows:

p.w.x: we use this command to run the input files of scf and nscf calculations of energy and wave functions at each and every k-points, which extracts the output files for the energy at eveiy k-points. Also it is used to calculate electronic structure, structural optimization, molecular dynamics.

ph,x: This command is used to calculate the phonon frequencies and displacement patterns, dielectric tensors, effective charges(using data produced by pw.x).

q2r.x: This code calculates the Interatomic Force Constants(IFC) in real space from dynamical matrices produced by ph.x on a regular q-grid.

matdyn.x: This codes helps in producing phonon frequencies at a generic wave vector using the IFC file calculated by q2r.x; which may also calculate phonon DOS.

pp.x: This extracts the specified data form files produced by pw.x , prepared data for plotting by writing them into formats that can be read by several plotting programs.

bands.x: This extracts the files from PWscf calculation and records its eigenvalues at different k-points with corresponding energies values ready for further processing. The code bands. x also performs the symmetry analysis of the band structure.

plotband.x: This codes reads the output files of bands.x, and then

produces band structure for PostScript plots.

dos.x: This command is used to calculate the electronic Density Of State (DOS) at different k-points.

projwfc.x: This code helps in calculating the projections of wave function over atomic orbitals s, p, d, f

CHAPTER FOUR

RESULTS AND DISCUSSION

The structural characteristics of the ground state configuration being examined of $KMnF_3$ and $SrMoO_3$ perovskites were carried out by firstly, optimizing the compounds structurally by minimizing the total energy of the compounds as regards to the variation of the lattice parameters. Both compounds have a cubic perovskite structure.

4.1 CRYSTAL STRUCTURES

The crystal structures of the two compounds ($KMnF_3$ and $SrMoO_3$) that were studied are shown below;

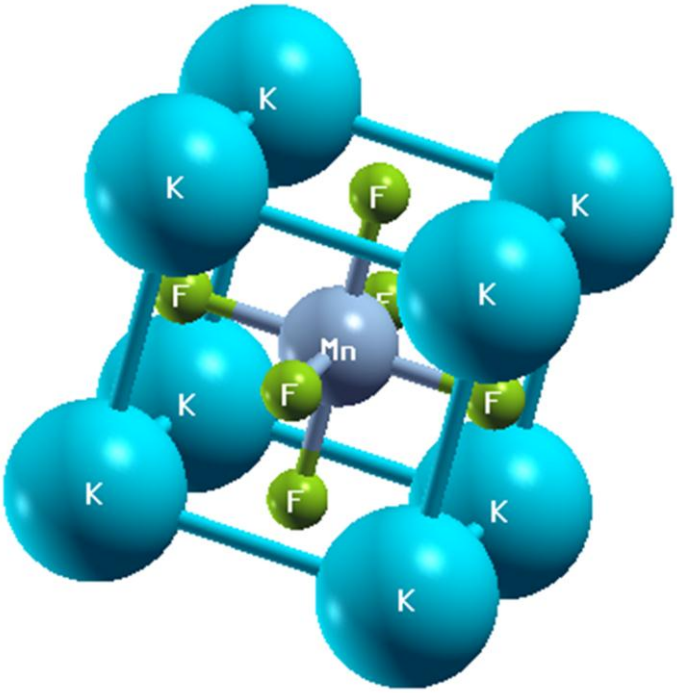

Figure 6: Crystal structure of $KMnF_3$

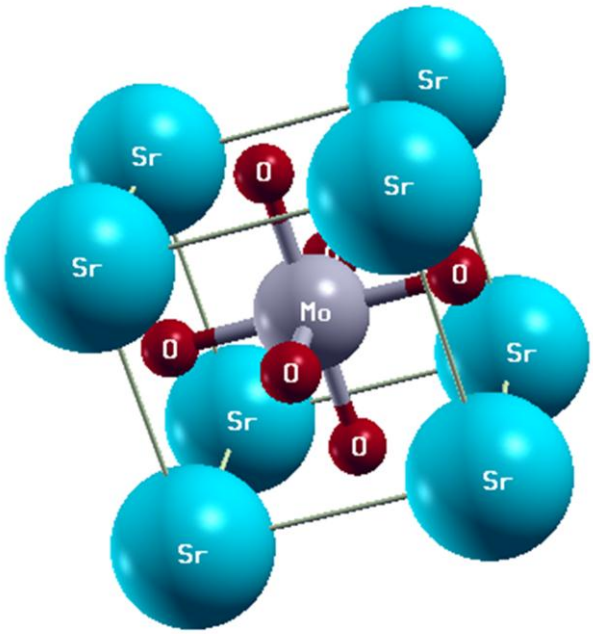

Figure 7: Crystal structure of $SrMoO_3$

4.2 BAND STRUCTURE GRAPHS

The electronic band structure of $KMnF_3$ and $SrMoO_3$ with their corresponding Density of States (DOS) is presented below:

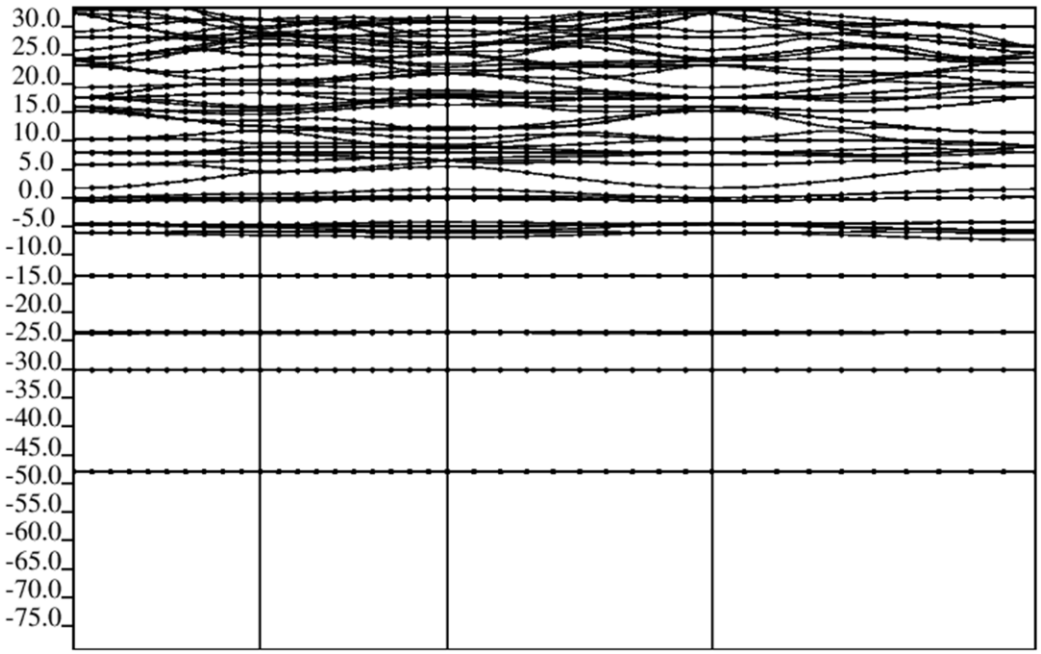

Figure 8: Band Structure of $KMnF_3$

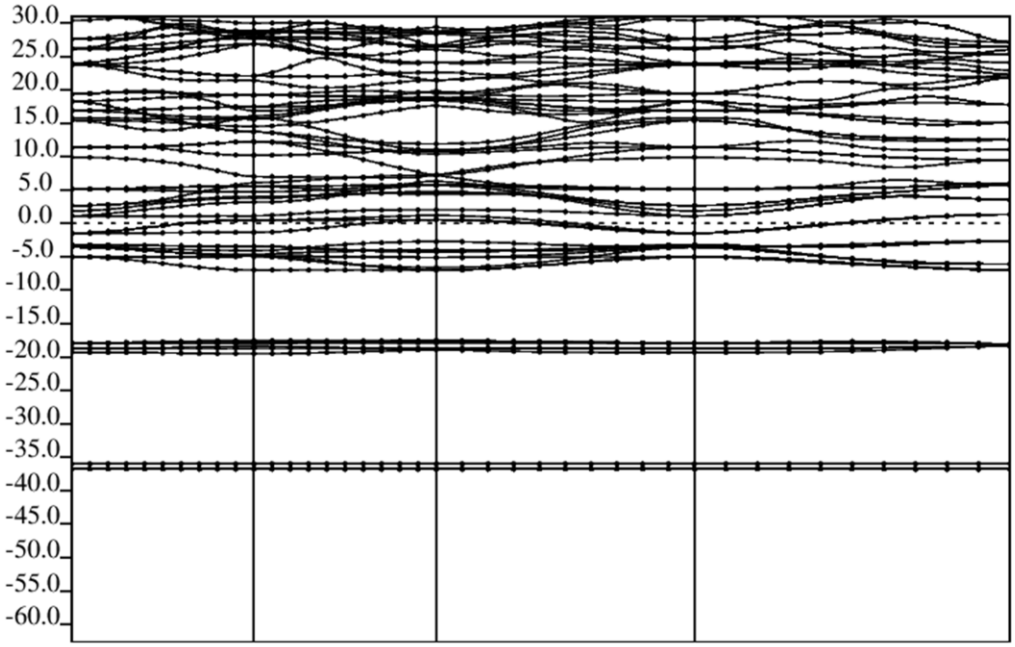

Figure 9: Band Structure of $SrMoO_3$

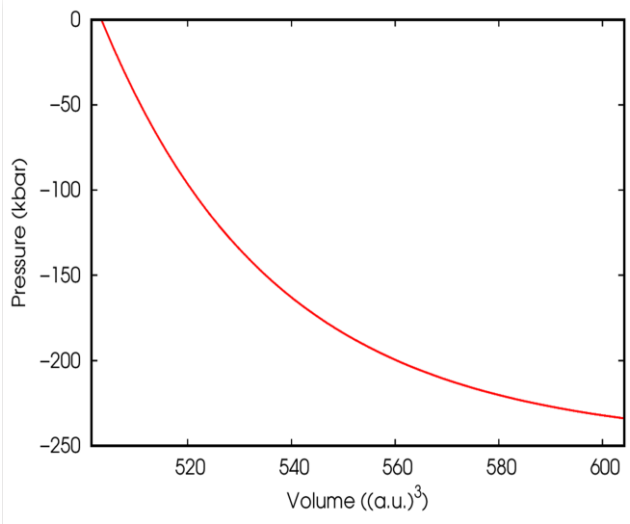

Figure 10a: Graph of pressure (kbar) against Volume (a.u.)^3 for $KMnF_3$

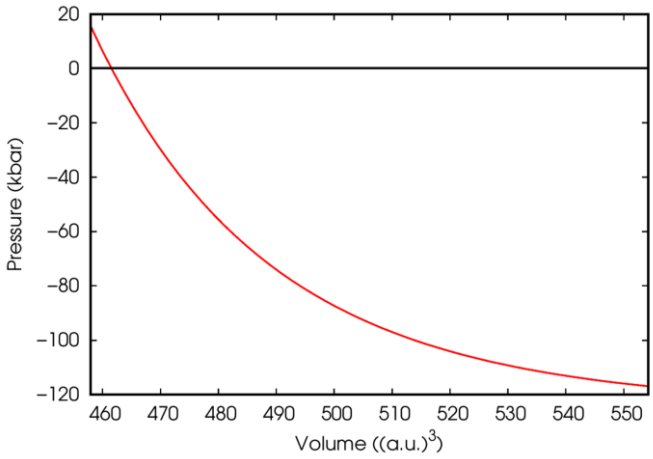

Figure 10b: Graph of pressure (kbar) against Volume (a.u.)^3 for $SrMoO_3$

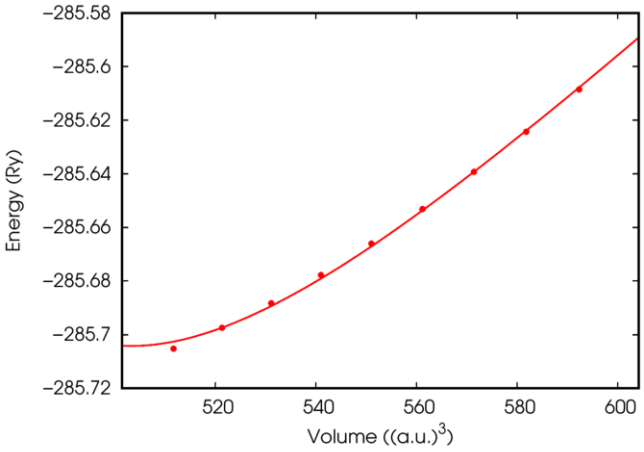

Figure 11a: Graph of Ennergy (Ry) against Volume (a.u)^3 for $KMnF_3$

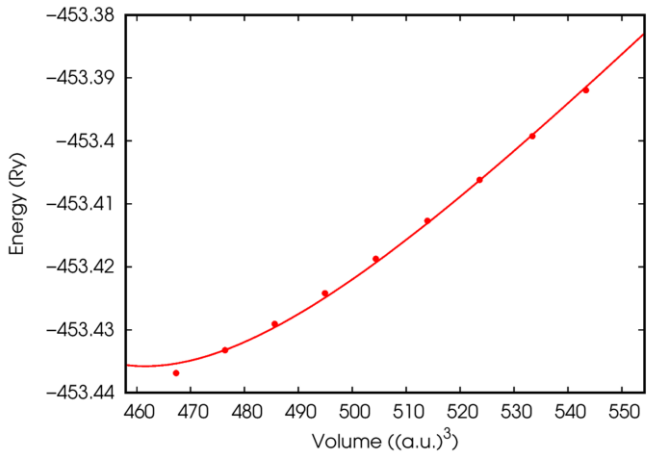

Figure 11b: Graph of Ennergy (Ry) against Volume (a.u)^3 for $SrMoO_3$

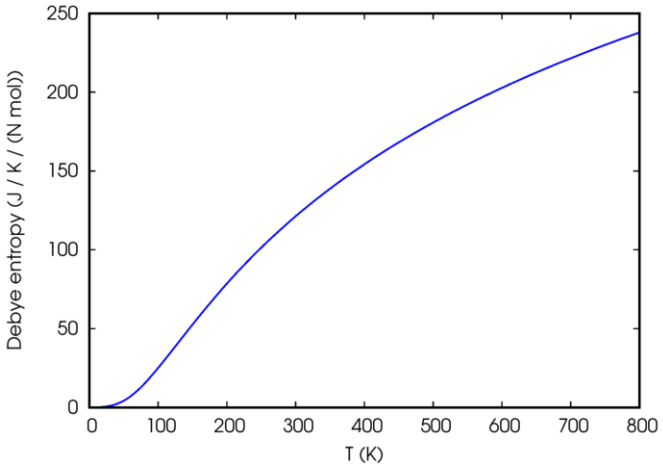

Figure 12a: Graph Debye Entropy C_v (J/K/N mol) against Volume (a.u.)^3 for $KMnF_3$

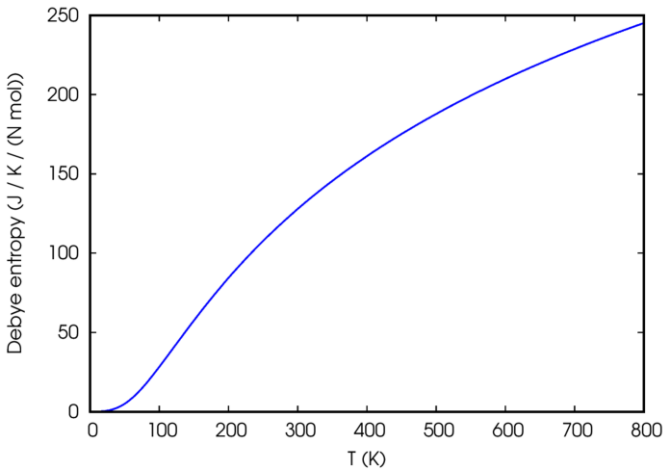

Figure 12b: Graph Debye Entropy C_v (J/K/N mol) against Volume (a.u.)^3 for $SrMoO_3$

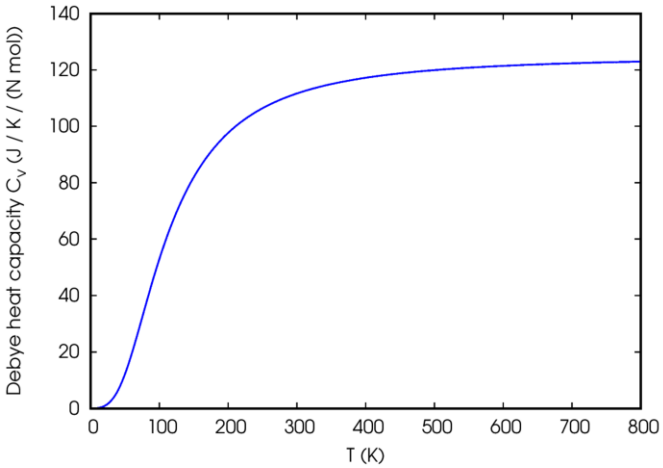

Figure 13a: Graph of Debye heat capacity C_v (J/K/N mol) against Volume (a.u.)^3 for $KMnF_3$

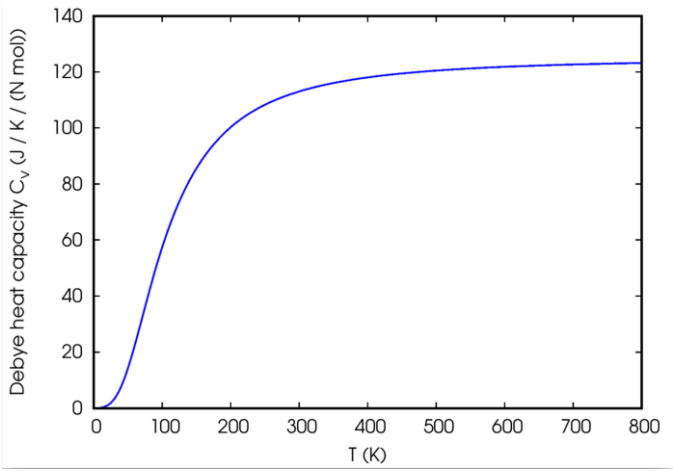

Figure 13b: Graph of Debye heat capacity C_v (J/K/N mol) against Volume (a.u.)^3 for $SrMoO_3$

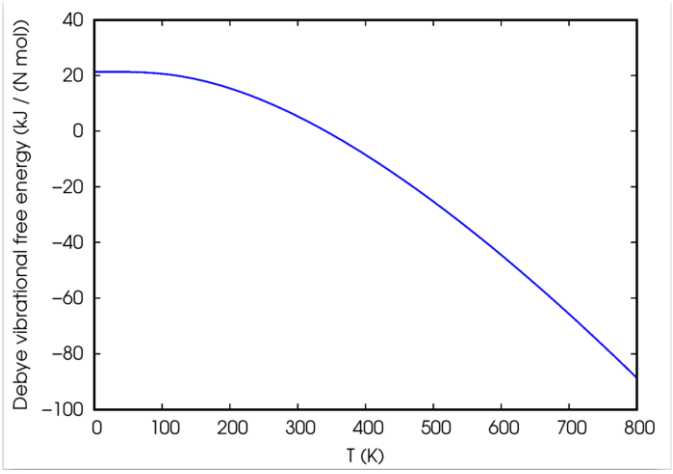

Figure 14a: Graph of Debye Vibrational free Energy (KJ/N mol) against Temperature (K) for $KMnF_3$

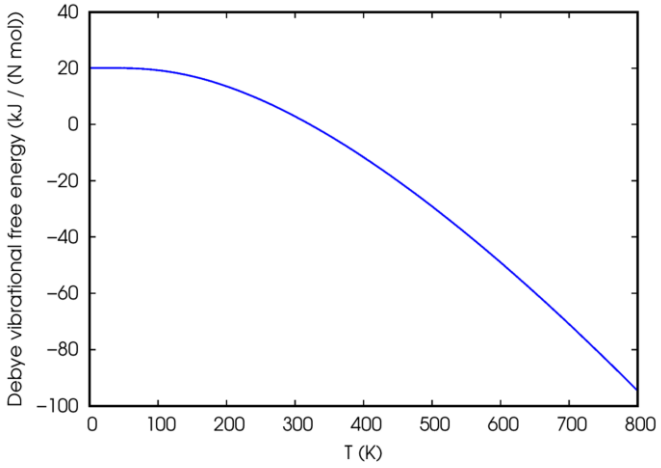

Figure 14b: Graph of Debye Vibrational free Energy (KJ/N mol) against Temperature (K) for $SrMoO_3$

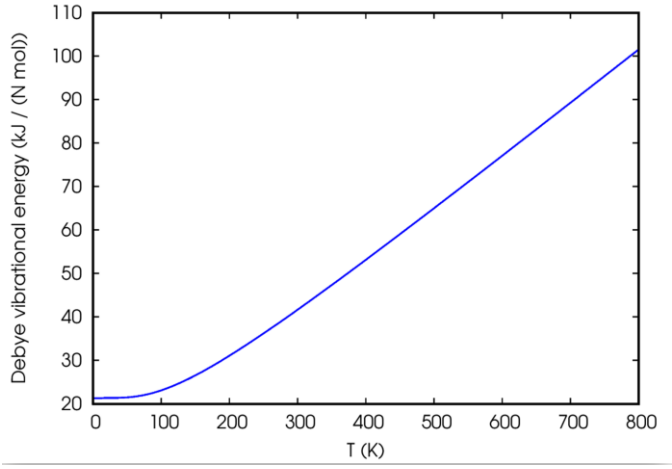

Figure 15a: Graph of Debye Vibrational Energy (KJ/N mol) against Temperature (K) for $KMnF_3$

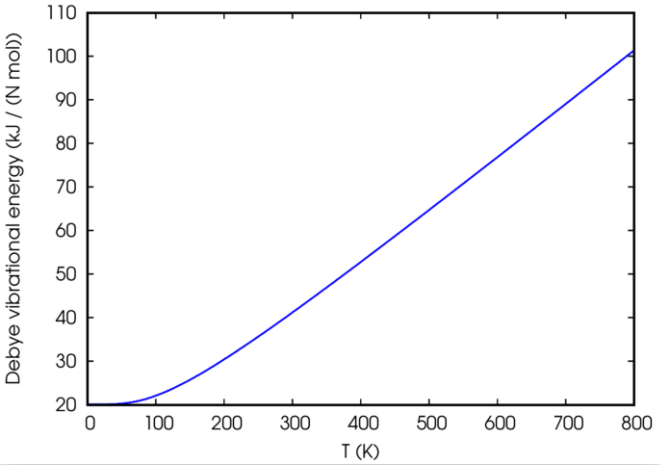

Figure 15b: Graph of Debye Vibrational Energy (KJ/N mol) against Temperature (K) for $SrMoO_3$

Table 4.1: Structural Properties of $KMnF_3$ and $SrMoO_3$

ALLOY	A	B	B'
$KMnF_3$	4.021	82.200	0.5629
$SrMoO_3$	3.998	182.500	0.154

MECHANICAL/ELASTIC PROPERTIES

Table 4.2: Mechanical Properties of $KMnF_3$ and $SrMoO_3$

Alloy	$KMnF_3$	$SrMoO_3$
C11	650.607	297.07
C12	254.515	150.49
C44	273.055	87.19
G	596.715	81.63
B/G	386.545	2.44
E	240.099	215.48
N	1.610	0.32
A	0.243	1.19
C12-C44	-18.540	492.745

4.3 DISCUSSION OF RESULTS

4.3.1 STRUCTURAL AND MECHANICAL PROPERTIES

To investigate the structural properties of the $KmnF_3$ alloys, firstly the structural optimization was carried out by minimizing the total energy of the alloys as regards the lattice parameters variation. The energy-lattice curves obtained for the various alloys using GGA are shown in chapter 3. By this optimization, the (lattice constants), B (Bulk modulus), B' (pressure derivative) of the alloys were obtained and presented in table 1. In solids, elastic constants play vital roles in determining the mechanical stability of the solid. For cubic phases, the stability is measured by the following criteria $C11+ 2C12 > 0$, $C44 > 0$, and $C11 > 0$. After the necessary investigations, the alloys were found to have satisfied all the above necessary conditions, therefore they can be said to be mechanically stable.

The Bulk Modulus (B), Young Modulus (E) and Shear Modulus (G) are parameters used to quantify the mechanical properties of solids. From tables 1 and 2, the results of the B, G and E show that the deformation resistance decreases in trend $KmnF_3$ – $SrMoO_3$ alloys. The B/G ratio is an experiential expression to establish the plasticity of a material. The threshold value for distinguishing between ductility and brittleness of materials is about 1.75. From our results, presented in Table 4.2, the alloys studied are ductile since their B/G

ratios are both greater than 1.75. The calculated results of Zener anisotropy (A), show that the alloys studied are anisotropic, since the values are greater than 1, which is an indication of very high anisotropy. These results were obtained using the relation:

$A= 2C44 \div C11-C12.$

Another factor that can affect the stability of a material against shear stress is the Poisson ratio 'n'. It shows the nature of the binding forces in materials. The value range is of the order $0 < n< 0.5$. From the results of 'n' in table 4.2, it shows that both alloys are of good plasticity. The Cauchy relation is another parameter which expresses the ductility and brittleness of materials. When its value is positive, the material is considered ductile, otherwise brittle. From table 4.2, it is obvious that the alloys under consideration are ductile.

4.3.2 ELECTRONIC PROPERTIES

Within the optimized stable crystal structure, we present the spin-polarized band structures and the density of states (DOS) of TaIrX (X= Ge and Sn) alloys as shown in figures 5 and 6. The exchange splitting between the minority-spin states is revealed in the Figures, and this is responsible for the asymmetry of the DOS.

CHAPTER FIVE

CONCLUSION

The first principle calculation was employed using quantum espresso program to determine the optimization, electronic band structure and mechanical properties of the perovskite compounds $KMnf_3$ and $SrMoO_3$. Our result show that the compound are conductors/metallic since valance and the conduction bonds crossed and giving rise to a zero energy gap.

REFERENCES

Aksel, Elena, Forrester, Jennifer S., Jones, Jacob L., Thomas, Pam A., Page, Katharine,

Atta, N.F., Galal, Ahmed, El-Ads, Ekram H., 2016. Perovskite nanomaterials – synthesis, characterization, and applications. Tech. Chapter 4, 108–151.

Bao, X., Wang, Y., Zhu, Q., Wang, N., Zhu, D., Wang, J., Yang, A., Yang, R., 2015. Efficient planar Perovskite solar cells with large fill factor and excellent stability. J. Power Sour. 297, 53–58.

Bhatti, Humaira Safdar, Hussain, Syed Tajammul, Khan, Feroz Alam, Hussain, Shahzad, 2016. Synthesis and induced multiferroicity of perovskite PbTiO3. Appl. Surf. Sci. 367, 291–306.

Bradley, Kathryn, 2017. Crystal Structure Prediction for Complex Modular Materials Doctor in Philosophy. University of Liverpool, p. 135.

Brockmann, T., 2009. Piezoelectric materials. In: Theory of Adaptive Fiber Composites. Springer, p. 205.

Chen, Yichuan, Zhang, Linrui, Zhang, Yongzhe, Gaoa, Hongli, Yan, Hui, 2018. Largearea perovskite solar cells – a review of recent progress and issues. RSC Adv. 8, 10489–10508.

Cheng, Z., Lin, J., 2010. Layered organic–inorganic hybrid perovskites: structure, optical properties, film preparation, patterning and templating

engineering. Cryst. Eng. Comm. 12, 2646–2662.

Christen, H.M., Eres, G., 2008. Recent advances in pulsed-laser deposition of complex oxides. J. Phys.: Condens. Matter 20 (26), 1–27.

Conings, B., Baeten, L., De Dobbelaere, C., D'Haen, J., Manca, J., Boyen, H., 014. Perovskite-based hybrid solar cells exceeding 10% efficiency with high reproducibility using a thin film sandwich approach. Adv. Mater. 26, 2041– 2046.

Deka, B., Ravi, S., Perumal, A., Pamu, D., 2014. Ferromagnetism and ferroelectricity in Fe doped BaTiO3. Physica B 448, 204–206.

Dhahri, Kh, Bejar, M., Dhahri, E., Soares, M.J., Graça, M.F.P., Sousa, M.A., Valente, M. A., 2014. Chemical physics letters blue-green photoluminescence in BaZrO 3I powders. Chem. Phys. Lett. 610, 341–344.

Di, Mei F., Falsi, L., Flammini, M., Pierangeli, D., Di, Porto P., Agranat, A.J., DelRe, E., 2018. Giant broadband refraction in the visible in a ferroelectric perovskite. Nat. Photo. 12, 734–738.

Dongling, Sun, Dongcai, Li, Zhiwen, Zhu, Jin, Xiao, Zetian, Tao, Wei, Liu, 2012. Photoluminescence properties of europium and titanium co-doped BaZrO3 phosphors powders synthesized by the solid state reaction method. Opt. Mater. 34, 1890–1896.

Eerenstein, W., Mathur, N., Scott, J.F., 2006. Multiferroic and magnetoelectric

materials. Nature 442, 759–765.

El-Ads, E.H., Galal, A., Atta, N.F., 2015. Electrochemistry of glucose at gold nanoparticles modified graphite/SrPdO3 electrode—towards a novel nonenzymatic glucose sensor. J. Electroanal. Chem. 749, 42–52.

electro -strain – polarization effect in La and Ni modified bismuth ferrite nanostructures. J. Alloy. Compd. 748, 504–514.

Feroze, Asad, Idrees, Muhammad, Kim, Deok-kee, Nadeem, Muhammad, Siddiqi, Saadat A., Shaukat, Saleem F., Atif, Muhammad, Siddique, Muhammad, 2017.

Francis, Nisha P., Dhanuskodi, S., Muneeswaran, M., Thomas, Anitta Rose, Giridharan, N.V., 2016. Optical nonlinearity in multiferroic bismuth ferrite. J. Alloy. Compd. 688, 796. Lu, H., Yang, G., Chen, Z., Dai, S., Zhou, Y., Jin, K., Cheng, B., He, M., Liu, L., Guo, H., 2004. Positive colossal magnetoresistance in a multilayer p–n heterostructure of Srdoped LaMnO3 and Nb-doped SrTiO3. Appl. Phys. Lett. 84, 5007. Garg, K., Nordblad, P., Heinonen, M., Panwar, N., Sen, V., Bondino, F., Magnano, E., Carleschi, E., Parmigiani, F., Agarwal, S., 2009. Study of Sb substitution for Pr in the Pr0.67 Ba0.33 MnO3 system. J. Magn. Magn. Mater. 321, 305–311.

Ghosh, Ayana, Trujillo, Dennis P., Choi, Hongchul, Nakhmanson, S.M., Alpay, S. Pamir, Zhu, Jian-Xin, 2019. Electronic and magnetic properties of

lanthanum and strontium doped bismuth ferrite: a first-principles study. Sci. Rep. 9 (194), 1–10.

Hatnean, Monica Ciomaga, Balakrishnan, Geetha, Haumont, Raphael, Martin, Romuald Saint, Velazquez, Matias, Maillard, Alain, Rytz, Daniel, Josse, Michael, Maglione, Mario, Kreisel, Jens, 2019. Single Crystal Growth of BaZrO3 from the melt at 2700 ————————————C using optical floating zone technique and growth prospects from BaB2O4 flux at 1350 ————————————C. Cryst. Eng. Comm. 21, 502.

Hodgson, E., 2013. Recent research activities on functional ceramics for insulator breeder and optical sensing systems in fusion reactors. J. Nucl. Mater. 442, S501–S507.

Hoefler, Sebastian F., Trimmel, Gregor, Rath, Thomas, 2017. Progress on lead-free metal halide perovskites for photovoltaic applications: a review. Monatshefte für Chemie – Chem. Month., 9 148 (5), 795–826.

Ishihara, T., 2009. In: Perovskite Oxide for Solid Oxide Fuel Cells, Fuel Cells and Hydrogen Energy. Springer Science Business Media, LLC, pp. 1–16 (chapter 1).

Jia, F., Zhong, H., Zhang, W., Li, X., Wanga, G., Songa, J., Cheng, Z., Yin, J., Guo, L., 2015. A novel nonenzymatic ECL glucose sensor based on perovskite LaTiO3-Ag0.1 nanomaterials. Sens. Actuat. B 212, 174–182.

Jia, Weiyi, Xu, W., Rivera, I., Pérez, A., Fernández, F., 2003. Effects of

compositional phase transitions on luminescence of Sr1 xCaxTiO3: Pr3+. Solid State Commun. 126, 153–157.

Jin, C., Cao, X., Lu, F., Yang, Z., Yang, R., 2013. Electrochemical study of Ba0.5Sr0.5Co0.8Fe0.2O3 perovskite as bifunctional catalyst in alkaline media. Int. J. Hydrogen Energy 38, 10389–10393.

Johnson, R.D., Radaelli, P.G., 2014. Diffraction studies of multiferroics. Annu. Rev. Mater. Res. 44, 269–298.

Kawamura, Y., Mashiyama, H., Hasebe, K., 2002. Structural study on cubic–tetragonal transition of CH3NH3PbI3. J. Phys. Soc. Jpn 71, 1694–1697.

Kézsmárki, I., Kida, N., Murakawa, H., Bordács, S., Onose, Y., Tokura, Y., 2011. Enhanced directional dichroism of terahertz light in resonance with magnetic excitations of the multiferroic Ba2 CoGe2 O7 oxide compound. Phys. Rev. Lett. 106.

Khajonrit, Jessada, Wongpratat, Unchista, Kidkhunthod, Pinit, Pinitsoontorn, Supree, Maensiri, Santi, 2018. Effects of Co doping on magnetic and electrochemical properties of BiFeO3 nanoparticles. J. Magnetism Mag. Mater. 449, 423–434.

Kim, J.K., Kim, S.S., Kim, W.-J., 2005. Sol–gel synthesis and properties of multiferroic BiFeO3. Mater. Lett. 59, 4006–4009

Kim, Jae-Sun, Yoon, Soon-Gil, 2000. High dielectric constant (Ba0.65Sr0.35) (Ti0.41Zr0. 59)O3 capacitors for gbit-scale dynamic random access

memory devices. J. Vac. Sci. Technol., B 18, 216–220.

Kleckers, Thomas, 2013. Electrical strain gauges, piezoelectric sensors or fiber Bragg sensors for force measurement: prospects and potentials. In: AMA Conferences- Sensor Proceeding, pp. 21–27.

Kreisel, J., Glazer, A., Jones, G., Thomas, P., Abello, L., Lucazeau, G., 2000. An X-ray diffraction and Raman spectroscopy investigation of A-site substituted perovskites compounds: the (Na1-xKx) 0.5Bi0.5TiO3 (0 x1) solid solution. J. Phys.: Condens. Matter 12, 3267.

Kumar, Praveen, Chand, Prakash, 2018. Structural, electric transport response and

Li, Hongjiao, Zhao, Y., Wang, Y., Li, Y., 2016. Sr2Fe2xMoxO6d perovskite as an anode in a solid oxide fuel cell: effect of the substitution ratio. Catal. Today 259 (2), 417–422.

Lianghao, Y., Yonghong, C., Qingwen, G., Dong, T., Xiaoyong, L., Guangyao, M., Bin, L., 2015. Layered perovskite oxide Y0.8Ca0.2BaCoFeO5+d as a novel cathode material for intermediate-temperature solid oxide fuel cells. J. Rare Earths 33 (5), 519–523.

Liu, H., Cao, B., O'Connor, C., 2011. Intrinsic magnetism in BaTiO3 with magnetic transition element dopants (Co, Cr, and Fe) synthesized by sol-precipitation method. J. Appl. Phys. 109, 07B516.

López-Juárez, Rigoberto, González, Federico, Villafuerte-Castrejón, María-

Elena, 2011. Lead-Free Ferroelectric Ceramics with Perovskite Structure. Ferroelectrics – Material Aspects. InTech Publisher, p. 518.

Low temperature synthesis and properties of BiFeO3. J. Electron. Mater. 46 (7), 4582.

Materialia 52 (3,9), 749–764.

Matthew, R., 2011. Monoclinic crystal structure of polycrystalline Na0.5Bi0.5TiO3. Appl. Phys. Lett. 98.

Morris, Madeleine Rachel, 2018. Barium Titanate: Photophysics, Photocatalysis & the Influence of the Ferroelectric Effect. A Doctoral Thesis, pp. 128

Mourachkine, Andrei, 2004. Room-Temperature Superconductivity. Cambridge International Science Publishing, Cambridge, UK, p. 307.

Nagata, S., Katsui, H., Hoshi, K., Tsuchiya, B., Toh, K., Zhao, M., Shikama, T.,

Neeraj, S., Kijima, N., Cheetham, A., 2004. Novel red phosphors for solid-state lighting: the system NaM (WO4)2–x(MoO4)x: Eu 3+(M- Gd, Y, Bi). Chem. Phys. Lett. 387, 2–6.

Nenasheva, E., Kanareykin, A., Kartenko, N., Dedyk, A., Karmanenko, S., 2004. Ceramics materials based on (Ba, Sr)TiO3 solid solutions for tunable microwave devices. J. Electroceram. 13, 235–238.

Nishihata, Y., Mizuki, J., Tanaka, H., Uenishi, M., Kimura, M., 2005. Self-regeneration of palladium-perovskite catalysts in modem automobiles. J. Phys. Chem. Solids 66 (2), 274–282.

Niu, Guangda, Guo, Xudong, Wang, Liduo, 2015. Review of recent progress in chemical stability of perovskite solar cells. J. Mater. Chem. A 3, 8970–8980.

Ohta, Hiromichi, Hiramatsu, Hidenori, 2018. Fabrication, characterization, and modulation of functional nanolayers. Part III. Nanoinformatics, 207–235.

Ono, Luis K., Juarez-Perez, Emilio J., Qi, Yabing, 2017. Progress on perovskite materials and solar cells with mixed cations and halide anions. ACS Appl. Mater. Interfaces 9, 30197–30246.

Ottochian, A., Dezanneau, G., Gilles, C., Raiteri, P., Knight, C., Gale, J.D., 2014. Influence of isotropic and biaxial strain on proton conduction in Y-doped BaZrO3: a reactive molecular dynamics study. J. Mater. Chem. A 2, 3127–3133.

Pecharsky, V.K., 2014. Magnetic and magnetothermal properties and the magnetic phase diagram of high purity single crystalline terbium along the easy magnetization direction. J. Phys. Condens. Matter. 26 (6). 066001.

Pena, M.A.; Fierro, J.L.G. Chemical structure and performance of perovskite oxides. Chem. Rev. 2001, 101, 1981. [CrossRef]

Pengfei, Fu, Shan, Qingsong, Shang, Yuequn, Song, Jizhong, Zeng, Haibo, Ning, Zhijun, Gong, Jinkang, 2017. Perovskite nanocrystals: synthesis, properties and applications. Sci. Bull. 62, 369–380.

Pinel, E., Boutinaud, P., Mahiou, R., 2004. What makes the luminescence of Pr3 +different in CaTiO3 and CaZrO3? J. Alloy. Compd. 380, 225–229.

Ponpandian, N., 2013. Novel synthesis of LaFeO3 nanostructure dendrites: a systematic investigation of growth mechanism, properties, and biosensing for highly selective determination of neurotransmitter compounds. Cryst. Growth Des. 13, 291–302.

Raghavan, V., 2015. Material Sciences and Engineering. PHL Learnt private Limited, Delhi, India, p. 463.

Ramesh, R., Spaldin, N.A., 2007. Multiferroics: progress and prospects in thin films. Nat. Mater. 6, 21–29.

Retot, H., Bessiere, A., Kahn-Harari, A., Viana, B., 2008. Synthesis and optical characterization of SrHfO3: Ce and SrZrO3: Ce nanoparticles. Opt. Mater. 30, 1109–1114.

Rojas-Cervantes, María Luisa, Castillejos, Eva, 2019. Perovskites as catalysts in advanced oxidation processes for wastewater treatment. Catalysts 9 (230), 1–38.

Roni, Peleg, 2018. The Perovskite Handbook. Metalgrass LTD, p. 108

Sayyadi-Shahraki, Ahmad, Taheri-Nassaj, Ehsan, Sharifi, Hassan, Gonzales, Justin, Kolodiazhnyi, Taras, Newman, Nathan, 2017. Origin of dielectric loss in Ba(Co1/3Nb2/3)O3 microwave ceramics. J. Am. Ceram. Soc. 101 (4), 1665–1676.

Schaak, R.E., Mallouk, T.E., 2000. prying apart Ruddlesden-Popper phases: exfoliation into sheets and nanotubes for assembly of perovskite thin films. Chem. Mater. 12, 3427–3434.

Science 358 (6364), 732–733.

Seyfi, B., Baghalha, M., Kazemian, H., 2009. Modified LaCoO3 nano-perovskite catalysts for the environmental application of automotive CO oxidation. Chem. Eng. J. 148, 306–311.

Shi, Zhengqi, Jayatissa, Ahalapitiya H., 2018. Perovskites-based solar cells: a review of recent progress, materials and processing methods. Materials 11 (5) 729– 743.

Singh, K., Maignan, A., Simon, C., Martin, C., 2011. FeCr2O4 and CoCr2O4 spinels: multiferroicity in the collinear magnetic state? Appl. Phys. Lett. 99.

Sorghum Millets 7, 393–420.

Spaldin, N.A., Cheong, S.W., Ramesh, R., 2010. Multiferroics: past, present, and future. Phys. Today 63, 38–43.

Szuromi, Phillip, Grocholski, Brent, 2017. Natural and engineered perovskites. Science 358 (6364), 732–733.

Szuromi, Phillip, Grocholski, Brent, 2017. Natural and engineered perovskites.

Tan, K.W., Moore, D.T., Saliba, M., Sai, H., Estroff, L.A., Hanrath, T., Snaith, H.J., Wiesner, U., 2014. Thermally induced structural evolution and

performance of mesoporous block copolymer-directed alumina perovskite solar cells. ACS Nano 8 (5), 4730–4739.

Taylor, Janet, Zhang, Ke, Wang, Donghai, 2019. Industrial and nonfood applications.

Thirumalairajan, S., Girija, K., Ganesh, V., Mangalaraj, D., Viswanathan, C.,

Tokura, Y., 2006. Critical features of colossal magnetoresistive manganites. Rep. Prog. Phys. 69, 797.

Tsunoda, Y., Sugimoto, W., Sugahara, Y., 2003. Intercalation behavior of nalkylamines into a protonated form of a layered perovskite derived from aurivillius phase Bi2SrTa2O9. Chem. Mater. 15, 632–635.

Wang, B., Gu, S., Ding, Y., Chu, Y., Zhang, Z., Ba, X., Zhang, Q., Li, X., 2012. A novel route to prepare LaNiO3 perovskite-type oxide nanofibers by electrospinning for glucose and hydrogen peroxide sensing. Analyst 138 (1), 362–367.

Wang, B., Gu, S., Ding, Y., Chu, Y., Zhang, Z., Ba, X., Zhang, Q., Li, X., 2012. A novel route to prepare LaNiO3 perovskite-type oxide nanofibers by electrospinning for glucose and hydrogen peroxide sensing. Analyst 138 (1), 362–367.

Wang, F., Li, C.-H., Zou, T., Liu, Y., Sun, Y., 2010. Electrically driven magnetic relaxation in multiferroic LuFe2O4. J. Phys.: Condens. Matter 22.

Wang, Jie, Shi, San-Qiang, Chen, Long-Qing, Li, Yulan, Zhang, Tong-Yi, 2004. Phasefield simulations of ferroelectric/ferroelastic polarization switching. Acta

Wang, Xudong, Zhou, Jun, Song, Jinhui, Liu, Jin, Ningsheng, Xu, Wang, Zhong ., 2006. Piezoelectric field effect transistor and nanoforce sensor based on a single

Wang, Y., Sun, Y., Zhang, J., Ci, Z., Zhang, Z., Wang, L., 2008. New red Y 0.85 Bi0.1Eu 0.05V1 yMyO4 (M= Nb, P) phosphors for light-emitting diodes. Physica B 403, 2071–2075.

Wenk, Hans-Rudolf, Bulakh, Andrei, 2004. Minerals: Their Constitution and Origin. Cambridge University Press, New York, NY, p. 413.

Whitfield, P.S., Herron, N., Guise, W.E., Page, K., Cheng, Y.Q., Milas, I., rawford, M.K., 2016. Structures, phase transitions and tricritical behavior of the hybrid perovskite methyl ammonium lead iodide. Sci. Rep. 6, 35685.

Xiao, Z., Ren, Z., Liu, Z., Wei, X., Xu, G., Liu, Y., Li, X., Shen, G., Han, G., 2011. Single crystal nanofibers of Zr-doped new structured PbTiO3: hydrothermal synthesis, characterization and phase transformation. J. Mater. Chem. 21, 3562–3564.

Xin, Cong, Veber, Philippe, Guennou, Mael, Toulouse, Constance, Valle, Nathalie,

Xu, B., Yin, K., Lin, J., Xia, Y., Wan, X., Yin, J., Bai, X., Du, J., Liu, Z., 2009. Room temperature ferromagnetism and ferroelectricity in Fe-doped BaTiO3. Phys. Rev. B 79.

Xu, Y., 2011. Ferroelectric Materials and Their Applications. Elsevier Publisher, p. 379.

Yagi, Shogo, 2009. KTN crystals open up new possibilities and applications vol. 7, 1–5.

Ye, Zuo-Guang, 2008. Handbook of Advanced Dielectric, Piezoelectric and Ferroelectric Materials: Synthesis, Properties and Applications. Elsevier, p. 1096.

Yi, Zijun, Ladi, Naji Haji, Shai, Xuxia, Li, Hao, Shen, Yan, Wang, Mingkui, 2008. Will organic–inorganic hybrid halide lead perovskites be eliminated from optoelectronic applications? (advance article) Nanosc Adv., 1276–1289 https://doi.org/10.1039/C8NA00416A.

Zhang, H., Fu, X., Niu, S., Xin, Q., 2008. Synthesis and photoluminescence properties of Eu3+-doped AZrO3 (A = Ca, Sr, Ba) Perovskite. J. Alloy. Compd. 459, 103–106.

Zhang, Yuqiao, Feng, Bin, Hayashi, Hiroyuki, Tohei, Tetsuya, Tanaka, Isao, Ikuhara, Yuichi, Ohta, Hiromichi, 2017. Thermoelectric phase diagram of the SrTiO3– SrNbO3 solid solution system. J. Appl. Phys. 121 (18).

Zhang, Z., Gu, S., Ding, Y., Zhang, F., Jin, J., 2013. Determination of hydrogen

peroxide and glucose using a novel sensor platform based on Co0.4Fe0.6LaO3 nanoparticles. Microchim. Acta 180, 1043–1049.

Zheludev, I.S., 2012. Physics of Crystalline Dielectrics: Volume 1 Crystallography and Spontaneous Polarization. Springer Science & Business Media, p. 375.

Zhou, D., Zhou, T., Tian, Y., Zhu, X., Tu, Y., 2018. Perovskite-Based Solar cells: materials, methods and future perspectives. J. Nanomaterials 2018,. 15 pages 8148072.

Zhu, J., Li, H., Zhong, L., Xiao, P., Xu, X., Yang, X., Zhao, Z., Li, J., 2014. Perovskite oxides: preparation, characterizations, and applications in heterogeneous catalysis. ACS Catal. 4, 2917–2940.

ZnO nanowire. Nano Lett. 6 (12), 2768–2772.

Zuo, Chuantian, Ding, Liming, 2017. Lead-free perovskite materials (NH4)3Sb2IxBr 9–x. Angew. Chem. Int. Ed. 56, 6528–6532.

Zverev, V.I., Tishin, A.M., Chernyshov, A.S., Mudryk, Y., Gschneidner Jr., K.A.,